Chapter 1

Introduction

This thesis examines the design of a mobile beacon for transmitting position location data. Many businesses require knowledge of current asset location. For example, rental car companies use Global Positioning System (GPS) trackers to determine the location of their vehicles, and some delivery companies use location beacons to track the timeliness of deliveries. In the interest of homeland security, some governments are requiring tracking devices on vehicles transporting hazardous materials. However, the Global Positioning System is not a communication system. GPS trackers consist of a GPS receiver to determine position and a communication system, which interfaces with the GPS unit. The communication system delivers the location information from the GPS receiver to the customer.

1.1 Problem Statement

Currently, many commercial beacons exist for transmitting GPS location data. However, many of these systems are large (over 2 cubic inches) and are inefficient, requiring input voltage levels in excess of 5 V for a lifetime of more than a few days. In fact, for extended device lifetime (a year or more), most commercially available devices require a permanent power source, such as a vehicle battery. For applications requiring a mobile tracking device, a permanent power source – or hardwired power – is unacceptable. For example, to track a cargo container from the ship to the dock to the trailer to the destination, a hardwired tracking device would be impractical.

This work aims to design a small, power efficient beacon for transmitting GPS location data for applications in which current commercially available beacons are impractical. Minimizing size is a design goal because smaller devices are easier to transfer between vehicles or containers. Maximizing power efficiency and minimizing power consumption are important for device portability and longevity. In the cargo container described above, it may take several weeks for the container to travel from the ship to its final destination, so the tracking device would have to last at least that long.

1.2 Satellite Systems

Several communications systems were considered for location data transmission, including several satellite communication systems. Satellites are classified by their orbital height: low earth orbit (LEO), medium earth orbit (MEO), and geostationary (GEO).

Geostationary satellites remain fixed over a point on the Earth's equator by orbiting the Earth at the same angular velocity as the Earth's rotation. Therefore, the orbital period of a geostationary satellite is equivalent to sidereal one day. The altitude required to achieve this orbital period is 35,786 km. Examples of satellite communication systems in geostationary orbit include imagery, television, and communication. The INMARSAT Satellite System is an example of a GEO satellite system and is discussed in Chapter 2.

Medium earth orbit (MEO) satellites have orbital altitudes between 1400 km and 35,780 km. MEO satellites are also referred to as intermediate circular orbit (ICO) satellites. The GPS satellites are considered MEO satellites, since their altitude is 20,200 km. The GPS system is briefly discussed in Chapter 4.

Low earth orbit (LEO) satellites have orbital altitudes between 200 km and 1200 km, which is the lowest usable range of orbital altitudes. LEO satellites – rather than GEO satellites – are often used for communication systems because they require lower transponder output power. Examples of LEO satellite systems include IRIDIUM and Globalstar, which are both discussed in Chapter 2. The Globalstar Satellite System was selected as the communication system for the transmission of the device location data. Reasoning for this choice is presented in Chapter 2.

1.3 System Overview

The system analyzed in this work consists of a transmitter, a channel, and a receiver. The goal of this work is to design a low power beacon – the transmitter – for the transmission of location data. The technical specifications of the beacon will be determined by simulating the performance of the receiver. The channel consists of the path from the beacon to the satellite to the receiver; the satellite has a linear transponder, so acts like a linear repeater.

The goal of the simulation is to determine the minimum required transmit power in order to correctly receive the signal. Once the minimum transmit power is determined, components can be selected to achieve the required power and efficiency. The determination of these components is left for future work.

Receiving a signal from the Globalstar Satellite System presents several challenges. Globalstar is a CDMA system, and the designed beacon will be transmitting at a power level significantly below other Globalstar signals. Therefore, the noise seen by the receiver will be very large compared to the desired signal, making signal acquisition difficult. Part of the noise seen by the receiver is from multiple access interference (MAI). MAI results when many users are trying to utilize the system at the same time; their signals add destructively with one another. The low received power level will result in a longer acquisition time, which is a design trade-off. Acquisition time will increase because the receiver will make more errors (false detections) when the power level is low. This effect is shown in Chapter 6 by examining the effects of different power levels at the receiver – as well as multiple users accessing the system – on the performance of the acquisition system.

1.4 Thesis Overview

This chapter provided an introduction to the work presented in the following chapters. Chapter 2 presents a feasibility study and evaluation of four different communication systems based on bandwidth availability and power requirements. Three of the communication systems

are satellite systems and the fourth system is based on cellular networks. As mentioned above, the Globalstar Satellite System was chosen for further development as a result of this study.

Chapter 3 presents a description of the Globalstar Satellite System. Each segment of the system is discussed, and the communication link is presented in detail. Concepts important to the operation of the Globalstar Satellite System, such as diversity, soft handoffs, and the Rake receiver are introduced. A link budget analysis is also presented as a basis for the simulation parameters. Differences between the single user case of the link budget and the more realistic multi-user case are discussed.

Chapter 4 discusses the technical concepts behind the Globalstar communication link. These concepts include direct sequence spread spectrum, the IS-95A cellular standard, and channel coding. An overview of the GPS communication subsystem is presented because of the parallel design challenges with the Globalstar satellite system. The GPS system utilizes spread spectrum to implement CDMA, and acquisition methods for CDMA systems are presented.

Chapter 5 provides an overview of a Globalstar transmitter and receiver, and then discusses the simulation design and how it differs from a Globalstar receiver. The results of the simulation are presented in Chapter 6. Two separate cases were tested to determine receiver performance: a single user accessing the transponder with an arbitrary signal time delay, and multiple users accessing the transponder also with arbitrary signal time delays. For the multiple user simulation, three different levels of satellite loading were considered: maximum loading (100% capacity), heavy loading (85% capacity), and average loading (50% capacity).

Chapter 7 discusses the results presented in Chapter 6 and their applications. Chapter 7 also discusses other simulations that should be investigated to further define the system.

Chapter 2

Feasibility Study

This feasibility study will determine the applicability of four communication systems to the improvement of a remote telemetry device. Only communication systems currently licensed for operation by the Federal Communications Commission (FCC) will be considered in this study due to time and cost constraints. The development of an improved remote telemetry device will expand the number of applications to which the device may be applied. The four communication systems are:

1. IRIDIUM Satellite System,
2. INMARSAT Satellite System,
3. Globalstar Satellite System, and
4. Using both a satellite system and a wireless network.

The remote telemetry device should satisfy the following conditions in order for the research to be fruitful. The conditions are listed in no particular order.

1. Already licensed for use (FCC, ITU, etc),
2. Small size,
3. Low power consumption.

The small size specification is to minimize the physical size of the transmitter. Ideally, the volume of the transmitter should be less than 5 cu. in., and measure no more than 5" on any one side. The low power consumption specification is given to maximize the battery life of the

device. The most important aspect of this optimization is current draw, but the supply and transmit voltages must also be minimized. Ideally, the required transmit power should be less than 1 W at a maximum. This thesis determines the minimum required transmit power. With this information, an optimization can be performed to minimize device power consumption; however, this optimization is not included in this thesis.

The purpose of this paper is to select one of the above systems for design consideration by evaluating each system against a set of common criteria. These criteria were chosen based on careful consideration of each of the desired conditions. The criteria are listed in ascending order, with the first item being the most important. The weights for each of the criteria are given following each item, as a percentage. The criteria are:

1. Power Consumption/Management – 60% (total)
    a. Consumption – 35%
    b. Management: Device should be programmable for settings such as transmission rate, sleep time, on time, etc. – 25%
2. Coverage Area – 30%
    a. Global coverage is preferred, but is not always available
3. Available bandwidth – 10%

Power consumption and management will be evaluated using the design criteria described above. *Coverage Area* describes the areas of the world in which a communication system is available for use. The available bandwidth of a communication system determines how many devices can be active in the system at the same time.

Each of the communication systems listed above will be summarized and then evaluated using these criteria. For the purpose of this study, it is assumed that device position information will be obtained via GPS. The systems will be discussed and then evaluated in the following order: IRIDIUM Satellite System, INMARSAT Satellite System, Globalstar Satellite System, and the case combining both satellite and wireless cellular technologies. If technical data on a transmitting device currently in the consumer market for each of these systems is available, an example of a working device for each system will be described.

2.1 IRIDIUM Satellite System

The IRIDIUM Satellite System consists of 66 polar orbiting satellites, a network of ground stations (10 world-wide), and personal communication devices. The IRIDIUM System is also configured to connect to the land-line infrastructure for Plain Old Telephone Services (POTS). When first conceived, the primary purpose of the IRIDIUM System was to provide a global telephone service [36]. However, for this paper and its applications, only Iridium's data services will be considered.

The 66 IRIDIUM Satellites are in Low Earth Orbit (LEO). The Iridium LEO satellites circle the globe at an altitude of approximately 780 km [36], and are much closer to the Earth than geostationary satellites. Because the IRIDIUM Satellites are polar orbiting, their orbits pass over both poles of the Earth – the North Pole and the South Pole. Given their proximity to the Earth, their velocity, and the velocity of the Earth's rotation, each satellite circles the globe in approximately 100.13 minutes, or just over an hour and a half. With 66 satellites in orbit, at least one satellite provides coverage to a given place 24 hours a day [17,18].

2.1.1 IRIDIUM Communication Subsystem

In any communication system design, it is critical to know the parameters of the system (and its limitations). The parameters of the Iridium Satellite Communication Subsystem are summarized in Table 2.1 below [17, 36]. These two sources differed slightly in their description of the system parameters. The values in [17] were arbitrarily selected when the parameter values differed. The IRIDIUM system utilizes both Time Division Multiple Access (TDMA) and Frequency Division Multiple Access (FDMA). FDMA allows the IRIDIUM system to reuse frequency bands between beams for larger capacity, and TDMA allows users to send and receive data over the system.

Uplink	1616 MHz
Downlink	1626.5 MHz
Bandwidth	10.5 MHz
Modulation Scheme (Links)	FDMA
Number of Channels	240
Channel Bandwidth	41.67 kHz
Guard Band	2 kHz
Modulation Scheme (Channels)	TDMA
Frame length	90 ms
User channels	8 (4 uplink, 4 downlink) per frame
Data Rates	
Full-duplex	4800 bps
Half-duplex	2400 bps
User channel time	8.6 ms

Table 2.1. IRIDIUM Communication System Parameters [17,36]

In the context of Table 2.1, a *channel* is utilized by users for transmitting and receiving data (in bursts). A *link* is a frequency channel that contains the user *channels*. The frequency channels (*links*) allow IRIDIUM to reuse frequencies to increase the system capacity.

2.1.2 Iridium Satellite Modem

The home page for the Iridium Satellite System (http://www.iridium.com) has links for several different types and brands of available devices. The modem discussed in this section was selected because it more closely approaches the goal of this research than the other available devices. The Model A3LA-DGS was designed by NAL Research Corporation of Manassas, VA; its specifications are discussed below in Table 2.2 [41].

Dimensions	7.7”x 3.3”x 1.5” (l x w x d)
Input Voltage	
Range	4 V_{DC} to 4.8 V_{DC}
Average	4.4 V_{DC}
Current (at 4.4 V_{DC})	
Standby	180 mA
Transmit	1 A
Data Call	550 mA
Power on	2.2 A (peak)
Operating Frequency	1616-1626.5 MHz
Duplexing	Time Division (TDD)
Multiplexing	TDMA/FDMA
Link Margin	13.1 dB
Data Rates	
Dial-up	2.4 kbps
Internet	10 kbps
Short-burst	1960 bytes per message
Short Message	160 characters

Table 2.2. Design Specifications of the Model A3LA-DGS Iridium Satellite Modem [41][1]

2.1.3 IRIDIUM System Evaluation

In this section, the IRIDIUM System will be evaluated using the criteria listed above: power, coverage area, and available bandwidth.

2.1.3.1. Power

The device described in Section 2.1.2 – The Model A3LA-DGS Iridium Satellite Modem – has the following power specifications [41]:

1. Standby Power: 0.57 W
2. Transmit Power: 4.4 W
3. Data Call Power: 2.2 W
4. Power-on Power (avg): 9.68 W

This device has a standby mode, but it is not clear if this mode is capable of being set remotely. The user can set the frequency of the data transmissions (at any time). Although the input voltage range is low, the transmit power (4.4 W) is greater than the design objective of no more

[1] Source: Reprinted with permission of NAL Research Corporation from [41]

than 1 W transmit power. The IRIDIUM Satellite System does not meet the power management criterion or the power consumption criterion.

2.1.3.2. Coverage Areas

As stated in Section 2.1, the IRIDIUM Satellite System is a global system, offering round-the-world coverage 24 hours a day. Like all satellite systems, IRIDIUM has limited capability under cover (for example, inside buildings or under thick canopy). However, the IRIDIUM Satellite System meets the criterion for available coverage.

2.1.3.3 Available Bandwidth

The IRIDIUM System has an available channel bandwidth of 41.67 kHz. Each frame is 90 ms long, but each user channel within that frame is only 8.6 ms long. However, at a data rate of 2.4 kbps, the available bandwidth should be sufficient; the IRIDIUM System meets the bandwidth criterion.

2.2 INMARSAT Satellite System

The first International Maritime Satellite Organization (INMARSAT) Satellite was launched in 1982. As with the IRIDIUM System, the primary purpose of the INMARSAT Satellite System was to provide global telephone coverage. Unlike the IRIDIUM System, the INMARSAT satellites are geostationary, with orbits at approximately 35,800 km above the Earth's surface [18]. One feature specific to geostationary satellites is that they revolve at approximate the same speed as the Earth's rotation rate. This feature allows a geostationary satellite to remain fixed over a specified point above the earth's equator. The INMARSAT System covers the globe with just four satellites, as opposed to Iridium's 66 satellites.

The four INMARSAT Satellites are positioned as follows: East Atlantic Ocean (AOR-E), West Atlantic Ocean (AOR-W), Indian Ocean (IOR), and Pacific Ocean (POR). The satellites are located at the following longitudes: AOR-E 15.5˚W, AOR-W 54˚W, IOR 64˚E, and POR 178˚E [32]. These positions and their spot beams are shown in Figure 2.1.

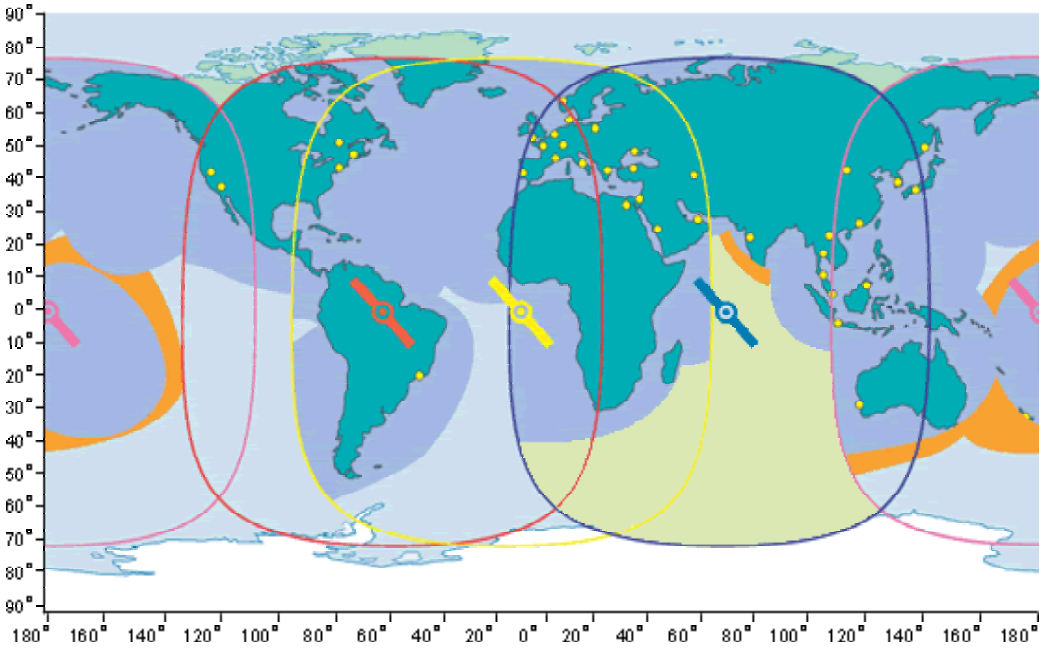

Figure 2.1. INMARSAT Satellite Coverage [31]

With these four satellites, INMARSAT currently offers several voice and data services. These services are categorized by their primary function. INMARSAT currently offers these services: Regional BGAN, GAN, M, C, and D+. Regional BGAN and GAN are global area networks – INMARSAT's newest venture. INMARSAT-M is their high-quality voice and data service, INMARSAT-C is a two-way data only service, and INMARSAT-D+ is a two-way short messaging and position reporting service. Since the purpose of this device is to transmit information data, the D+ link will be utilized.

2.2.1 INMARSAT-D+ Communication Subsystem

The only data found describing the INMARSAT-D+ Communication link is part of the DMR-200 D Specification Sheet [48]. The INMARSAT-D+ Communication link is described in Table 2.3. In [32], the author gives a range of transmit data rates between 4 bps and 128 bps.

Frequency Range	
Receive	1525 – 1559 MHz
Transmit	1626.5 – 1660.5 MHz
EIRP	0 – 9 dBW
Elevation Angle Range	15 – 90°
Modulation	
Forward Channel	32-ary FSK, 20 bps
Reverse Channel	binary FSK, 4-128 bps
Forward Error Correction	
Forward Channel	Reed-Solomon(31,15)
Reverse Channel	½-rate convolutional (k=7)
Message Length	
Forward Channel	64 bits (burst)
Reverse Channel	200 digits (max), or 133 characters (max)

Table 2.3. The INMARSAT-D+ Communication Design Specifications [32, 48]

2.2.2 DMR-200 D

Skywave Mobile Communications, in cooperation with SkyNet Mobile Communications offers several devices for use with the INMARSAT-D+ service. The DMR-200 D was selected because it is widely used in the tracking industry. More information on this device and other available devices and services from Skywave Mobile can be found at their website, www.skywavemobile.com. The technical specifications – available on the Skywave website – are summarized in Table 2.4 [48].

Dimensions (dia x h)	6.3” x 2”
Input Voltage	9 VDC to 30 VDC
Power Consumption (@ 12 V_{DC})	
Receive	0.9 W
Idle	0.25 W
GPS Active	1 W
Heater Active	5 W
Transmit	10 W
Sleep	6 µW (500 µA)

Table 2.4. DMR-200 D Technical Specifications [48][2]

[2] Source: Reprinted with permission of SkyWave Mobile [48]

2.2.3 INMARSAT System Evaluation

In this section, the INMARSAT System will be evaluated using the criteria listed in the Introduction.

2.2.3.1 Power

The device, the DMR-200D, has a required input voltage ranging from 9 - 30 VDC. At 12 VDC, the DMR has a transmit power of 10 W, which is much greater than the power level required for this thesis. The DMR does not meet the power consumption criterion. However, the frequency of the DMR-200D's data transmissions can be set remotely; the DMR-200D meets the power management criterion.

2.2.3.2 Coverage Areas

As stated in Section 2.1, the INMARSAT Satellite System is a global system, offering effective global coverage 24 hours a day. Like all satellite systems, INMARSAT has limited capability under cover (i.e. inside buildings, under thick canopy). However, the INMARSAT Satellite System meets the criterion for available coverage.

2.2.3.3 Available Bandwidth

The INMARSAT D+ System bandwidth specifications were not readily available. The stated data rate range of 4 – 128 bps is very wide. Due to the lack of information, the INMARSAT D+ system does not meet the bandwidth criterion.

2.3 Globalstar Satellite System

The Globalstar Satellite System utilizes a low earth orbit constellation. There are 48 satellites in the constellation orbiting at 1414 km. (At 900 km, there are four additional satellites, which are spares.) These 48 satellites provide service between ±70˚ latitude; however, a ground station (gateway) is required to utilize the service [24, 51]. Globalstar was the last of the three satellite systems presented here to offer service – beginning in late 1999.

The Globalstar system uses Code Division Multiple Access (CDMA) for its communication waveforms, but the satellite transceivers are "bent-pipe", meaning no data processing is done by the satellite. All data processing is completed by the terrestrial gateways. The Globalstar system was intended to extend the existing terrestrial telephony systems, and was designed to interact with the terrestrial infrastructure. Because of this, many subscriber units have the capability to operate on either the satellite link or a *compatible* cellular link. This capability will be explored in Section 3.4.

2.3.1 Globalstar Communication Subsystem

As typical with other published satellite communication system parameters, several of the Globalstar sources contradict each other. Preference is given to [24] as it is the more recent document. The link parameters are summarized in Table 2.5.

User to Satellite:	
Uplink	1610-1626.5 MHz
Downlink	2483.5-2500 MHz
Gateway to Satellite:	
Uplink	5091-5250 MHz
Downlink	6875-7055 MHz
Spot Beam	5760 km (diameter)
Modulation Scheme (Links)	FDM
Number of Channels	13
Channel Bandwidth	1.25 MHz
Modulation Scheme (Channels)	CDMA
Number of Beams	16
Beam Footprint	~1150 km (diameter)
Honeycomb pattern	

Table 2.5. Globalstar Communication System Parameters [24][3]

2.3.2 Axonn AXTracker

The home page for the Globalstar Satellite System (www.globalstarusa.com) has links for several different types and brands of available devices. The modem discussed in this section was selected because it more closely approaches the goal of this research than the other available devices. The AXTracker was designed by Axonn, LLC, and incorporates AeroAstro's simplex modem. Technical specifications of the AXTracker were unavailable, but the specifications of AeroAstro's modem were available. The specifications for the AeroAstro modem are discussed below in Table 2.6 [21, 24].

Dimensions	3" x 3" x 0.75" (l x w x d)
Input Voltage	5 V_{DC} ± 5%
Current (at 5 V_{DC})	
Transmit	0.5 A (typ)
Sleep	6 µA
Transmit Frequency	1610-1620 MHz
Transmit EIRP	159 mW (min)
Data Rate	100 bps (uplink)

Table 2.6. Design Specifications of the AeroAstro Simplex Modem for the Globalstar Satellite System [21][4]

[3] Source: Reprinted with permission of Globalstar, Inc. from [21]
[4] Source: Reprinted with permission of AeroAstro, Inc. from [21, 24]

The AXTracker receiver that interfaces with the Globalstar ground stations costs approximately $500,000. The development of a lower cost receiver would greatly benefit customers.

2.3.3 Globalstar System Evaluation

In this section, the Globalstar System will be evaluated using the criteria listed in the Introduction. This evaluation is based on the AeroAstro Simplex Modem specifications.

2.3.3.1 Power

In transmit mode, the modem uses 2.5 W, and in sleep mode, the current draw is negligible. Although this transmit power is slightly higher than desired, it is close to the desired transmit power. It can be assumed that the transmit power can be reduced through design optimization; the modem meets the power consumption criterion. The rate of data transmissions is programmable by the user, but it is unclear if the rate is remotely programmable. The modem meets the power management criterion.

2.3.3.2 Coverage Areas

As stated in Section 2.3.1, the Globalstar Satellite System is a global system, offering round-the-world coverage 24 hours a day. Like all satellite systems, Globalstar has limited capability under cover (for example, inside buildings or under thick canopy). However, the Globalstar Satellite System meets the criterion for available coverage.

2.3.3.3 Available Bandwidth

The Globalstar channel bandwidth is 1.25MHz, and the Aero-Astro modem data rate is 100 bps. This is a rather low data rate, but the bandwidth is sufficient. The modem meets the criterion for available bandwidth.

2.4 Combining Wireless and Satellite Cellular Technology

The satellite communication systems discussed in this study were each originally designed for telephony services. As part of this design, each system is capable of interacting with either the landline telephone system or a cellular system. Globalstar subscriber units were originally designed to allow the user to access either the local cellular network or the satellite network. This section discusses one specific application of using GSM / PCS cellular networks to deliver GPS satellite network information.

2.4.1 Discussion

The current cellular networks are complex and varied. For this study, two specific networks are investigated: the Personal Communication Services (PCS) network (1900 MHz) and the Global System for Mobile (GSM) communication network (900/1800 MHz). These two services together provide cellular service worldwide. Figure 2.2 shows the GSM world coverage, and Figure 2.3 shows the PCS world coverage. [49] In both figures, the darkened or shaded areas indicate where coverage for that service is currently available.

Although cellular coverage is concentrated in the populated areas of the world, cellular communication systems are important to consider. Cellular communication systems can often work where satellite communication systems cannot, such as indoors or under heavy cover. Combining a Globalstar modem with a GSM device – such as the Trimtrac – would be an interesting topic for investigation. However, developing such a device would require a significant amount of time and money.

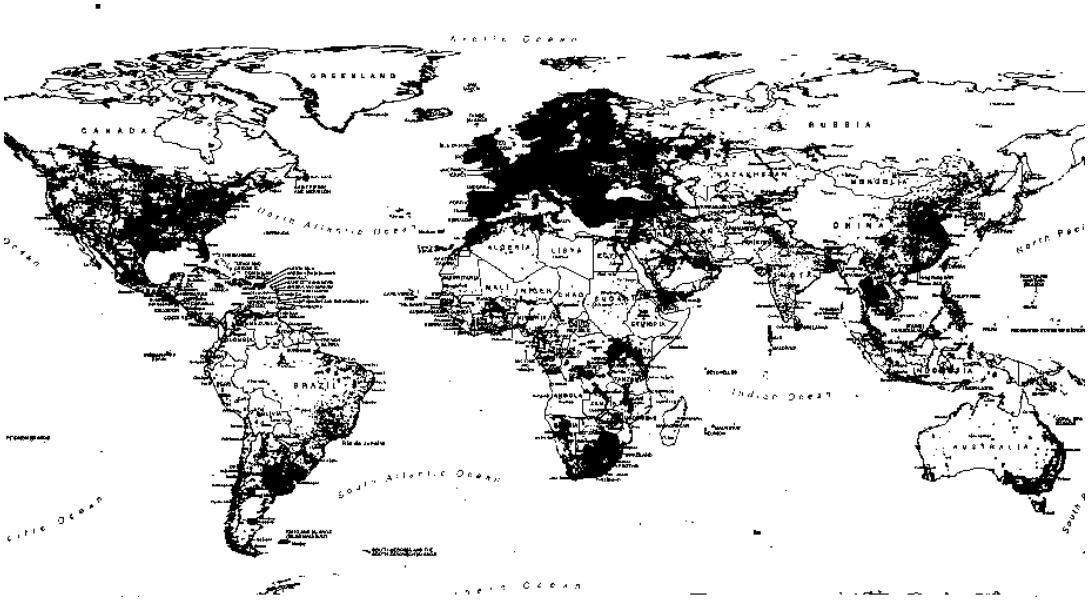

Figure 2.2. GSM Worldwide Coverage. Darkened areas indicate available service. (From [14], © 2006 Europa Technologies, Ltd.)

Figure 2.3. PCS Worldwide Coverage – Shaded areas indicate available service. (From Figure 1 of [49], © 2006 Sprint Nextel. Reproduced with permission.)

2.4.2 The Trimtrac by Trimble.

The Trimtrac is a compact location device produced by Trimble (www.trimtrac.com). The Trimtrac contains a GPS receiver for determining the location of the device and a cellular RF section for transmitting data via the cellular network. The Trimtrac RF section can transmit

on three different carrier frequencies, allowing it to interface with either the GSM cellular network or the PCS cellular network. The batteries and antenna are both internal to the device (see dimensions below). The datasheet claims 90 days of operation on 4 AA batteries, but does not specify the reporting rate to achieve that battery life. All specifications are taken from the Trimtrac datasheet [52].

Dimensions	5.78" x 2.99" x 1.44" (l x w x h)
GSM /PCS	Data only
Frequency	900/1800/1900 MHz
Transmit Power	
900 MHz	2W
1800/1900 MHz	1W
GPS	
Frequency	1575.42 MHz, C/A code
Acquisition	
Signal Power	-130.0 dBm
Hot Start (50%)	< 24sec
Warm Start (50%)	< 38sec
Cold Start (50%)	< 90sec

Table 2.7. Trimtrac Technical Specifications [52]

2.4.3 Evaluation of a combined Wireless & Satellite Communications System

In this section, the combined wireless and satellite system (GSM/PCS and GPS) will be evaluated using the criteria listed in the Introduction. This evaluation is based on the Trimtrac specifications.

2.4.3.1 Power

Depending on the network used, the Trimtrac uses between 1 - 2 W for transmission. The specifications do not include the power required by the GPS module, which could be quite significant depending on the placement of the device and the rate of transmissions. Due to these unknowns, the Trimtrac does not meet the power consumption criterion. Although the datasheet [52] specifies *on-demand polling*, this feature does not imply a power management scheme. On-demand polling allows a user who is not at the same location as the device to *poll* (or request) the device for its current location via the communication infrastructure. This type of data retrieval requires two-way communications between the system receiver and the transmitter. In other

words, the transmitter must also be able to receive and process data from a ground-station or base-station. The Trimtrac meets the power management criterion.

2.4.3.2 Coverage Areas

Although the GSM/PCS networks claim to be global, they are not truly global. As shown in Figures 2.2 and 2.3, cellular network access is available only in populated areas. Although GPS is a truly global system, data can only be retrieved when the device is able to connect to the cellular network.

2.4.3.3 Available Bandwidth

The total bandwidth available to the GSM network is 25 MHz. This bandwidth is divided into 200 kHz wide channels. The total bandwidth available to the PCS network is much higher at 140 MHz. Therefore, the both the GSM and PCS cellular networks satisfy the bandwidth requirement.

2.5 Conclusions and Recommendations

This feasibility study has considered four communication systems – Iridium, Inmarsat, Globalstar, and GSM – and evaluated each system against a set of common criteria. The results of the evaluations are summarized in Table 2.8.

	IRIDIUM	INMARSAT	Globalstar	GSM/GPS
Power (60%)	No	--	Yes	--
Management (25%)	No	Yes	Yes	Yes
Consumption (35%)	No	No	Yes	No
Coverage (30%)	Yes	Yes	Yes	No
Bandwidth (10%)	Yes	No	Yes	Yes
TOTAL	40%	75%	100%	35%

Table 2.8. Feasibility Study Evaluation Results.

Table 2.8 shows that the Iridium and Globalstar Satellite systems satisfy the evaluation criteria, and the Inmarsat Satellite system and the GSM Cellular systems do not satisfy the evaluation criteria. All systems (expect Globalstar) were evaluated using devices containing both a communications module and a GPS module. Changing the GPS module or programming in any of these devices would likely result in better power consumption performance.

Both the Iridium and Globalstar systems would satisfy the requirements for this study. However, the Globalstar system will be investigated in further detail due to the availability of information and ease of obtaining a device. If for some reason the Globalstar system fails to meet the design criteria after further investigation, the Iridium system will be investigated for design of the beacon.

Chapter 3

The Globalstar Satellite System

The Globalstar Satellite System has three separate segments: the satellite segment, the ground station segment, and the user device segment. Figure 3.1 shows an overview of the Globalstar Satellite System. The forward link describes the complete link from the gateway to the satellite to the user terminal. The reverse link describes the complete link from the user terminal to the satellite to the gateway. Communications originating from the satellite are referred to as the downlink, and communications originating from the ground are referred to as the uplink.

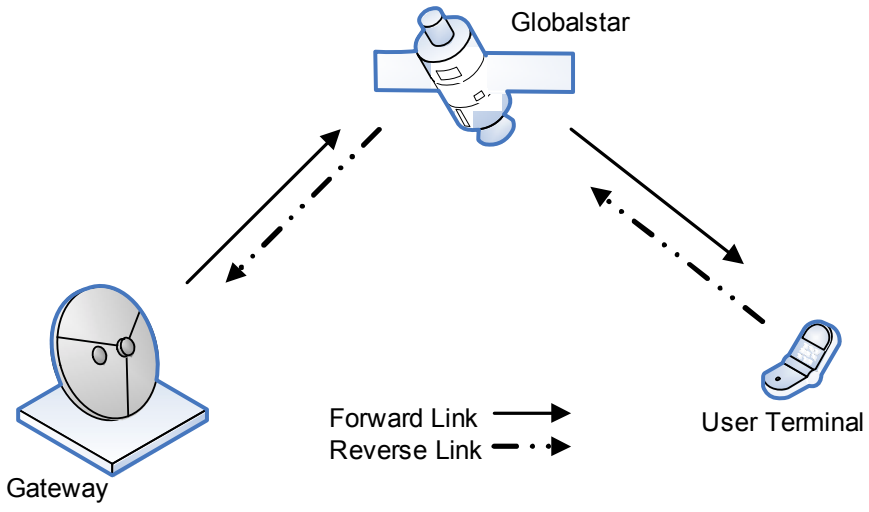

Figure 3.1. The Globalstar Satellite System Model

The Globalstar System is primarily a voice communication system, providing users with a satellite-based cellular communication system. Although primarily a voice system, the Globalstar System can also be used to transmit and receive data at low data rates. This thesis discusses an application of the Globalstar system in which data are transmitted from a beacon at a remote location to the receiver at the ground station. In the Globalstar Satellite System, the ground stations are referred to as *gateways*.

3.1 Globalstar System Overview

Each segment of the Globalstar System will be discussed and a link budget will be presented. Some unique characteristics of the Globalstar System, such as the waveform, the power management scheme and soft hand-offs are discussed in detail. Additionally, the Axonn AXTracker will be discussed as an illustration of a Globalstar communication device for transmitting data.

3.1.1 The Satellite Segment

The satellite segment consists of 48 low-earth orbiting satellites organized into 8 orbital planes. The constellation was designed to provide coverage between 70˚ N and 70˚ S latitudes with a view of at least 2 satellites at an elevation greater than 10˚ from any point in the service region. The coverage is achieved through the satellite constellation design. Globalstar has achieved this goal, although some sources cite degraded system performance near the equator and near the edges of the coverage region. Most users in the coverage area are within the footprint of 2 to 4 Globalstar satellites, allowing for the soft-handoffs discussed later. Some of the parameters of the satellite segment are summarized in Table 3.1 below [11,18].

Parameter	Value
Orbital Height	1414 km
Orbital Period	114 minutes
Average Pass duration	10-15 minutes
Footprint Diameter	3600 miles (5793.6 km)
Number of Beams	16

Table 3.1. Globalstar Satellite System Parameters [11]

In Table 3.1, the *Orbital Height* is the altitude of the satellite above the surface of the earth, and the *Orbital Period* is the amount of time required for one satellite to make a full revolution around the earth. Since the Globalstar Satellite System is a polar system, this parameter refers to the time for a satellite to make a full revolution around the earth's poles. The *Average Pass Duration* refers to the average length of time a single satellite can be seen from a single point on the earth's surface. Even though the satellite is in view for this period of time, a receiver may not detect a signal from the satellite for the entire period. This is because the signal strength from the satellite is severely degraded when the satellite is less than 10˚ above the horizon.

The *Footprint Diameter* refers to the diameter of the area on the surface of the earth as seen by the satellite. In this thesis, the satellite footprints will be modeled as approximately circular. Another method of defining a satellite's footprint is by the beamwidth. Typically, both horizontal and vertical beam widths are required to define a satellite's footprint; these values represent the width (horizontal) and height (vertical) of the footprint in degrees. Beamwidths are discussed in more detail in Section 3.2.2.

3.1.2 The Ground Segment

The ground segment consists of 24 gateways across the globe. In the Globalstar Satellite System, the ground stations are called *gateways*. Gateways (or ground stations) communicate with user devices via the satellites and are often used to manage both system resources and user devices and accounts. Gateways are typically fixed transceivers with a large antenna for transmitting and receiving. Sometimes, gateways have several large antennas to increase system capacity. A generalized block diagram of a Globalstar gateway is shown in Figure 3.2. The gateway consists of a communications block, a routing and processing block, and an interface to other telecommunication networks, such as the public-switched telephone network (PSTN) and

other cellular networks. (Some publications separate the telecommunication interface into a fourth segment.) The communications block can be broken down into an antenna (or a group of antennas) and the corresponding controller(s), and a transceiver. For the link budget calculation in Section 3.2.2, it is important to note that the gateway antennas are approximately 6 meters in diameter [11].

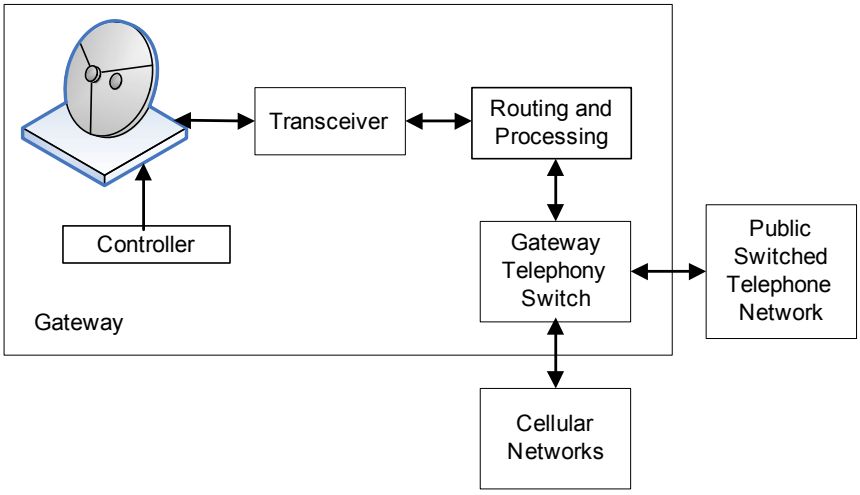

Figure 3.2. Globalstar gateway block diagram [11]

Because the Globalstar satellites do not process data, all the data processing is done at the gateways. Each gateway can provide up to 119 traffic channels within the forward channel. The channel in this case refers to the 1.23 MHz frequency division bandwidth, which is discussed in Section 3.2. This bandwidth (1.23 MHz) also corresponds to the bandwidth of the spread data (1.228 MHz). In a CDMA system, all of the channels (119 in this case) are transmitted in the same bandwidth and at the same frequency. The gateways also control system access and security as well as track usage and billing for all customers. Each gateway can perform these tasks only within its own footprint, so the gateways are interconnected via the existing PSTN system to enable a seamless communication network: the Globalstar network [46].

Although there are 24 Globalstar gateways worldwide, there are currently only 4 gateways equipped to process data communications. The data communication module licensed for use on the Globalstar System is a simplex modem. This modem transmits at a much lower power level and bit rate than the Globalstar telephones, thus requiring a special module at the

gateway to receive and process the modem data [21]. As described in Section 2.3.2, this receiver module costs approximately $500,000.00, which is a substantial investment for any user.

3.1.3 The User Device Segment

There are several variations of user devices available, including handheld and fixed phones, data communication equipment, and aviation and marine rated equipment. Current user handheld phones are about the size of a land-line cordless phone without the satellite antenna. The detachable satellite antenna is a thin cylinder nearly the same length as the phone. The satellite antenna is detachable because most current handheld phones will operate on both satellite and cellular networks. User terminals incorporate Rake receivers to enhance performance, and have an average transmission EIRP of -10 dBW [11]. A Rake receiver enhances system performance by constructively combining multipath signal components; Rake receivers are described in detail in Section 4.1.2.

There are two modems certified for use on the Globalstar System: a simplex modem and a duplex modem. Aero-Astro produces the simplex modem licensed for use on the Globalstar Satellite System. This modem requires an external antenna and power source, provides transmit only capabilities, and has very little power saving capability. Aero-Astro provides online access to simplex modem data for registered users. Table 3.2 summarizes the technical specifications of the Aero-Astro Simplex Modem [21].

Input Power	5 V (500 mA)
Data Rate	100 bps
Standby Power	6 μA
Alert Power (Receiver on)	75 mW
Waiting Power (between transmissions)	1 mW
Transmission Power	2.5 W
Transmission Duration	1.36 sec
Dimensions	3” x 3” x 0.75”

Table 3.2. Aero-Astro Simplex Modem Technical Specifications [21]

In Table 3.2, the Transmission Duration is the length of time required to transmit the data sequence, and is sometimes referred to as the pulse length. The *Alert Power* is the power consumed when the receiver is on, the *Standby Power* is the power consumed when the modem

is in standby mode. In standby mode, the modem shuts down most of its components for a specified length of time to conserve battery power. The Aero-Astro Globalstar modem has several programmable settings, which may be either specified by the user or left as defaults. The programmable settings include:

- Maximum/minimum intervals between transmissions,
- Number of transmission attempts, and
- GPS data included.

As stated in Table 3.2, the Aero-Astro modem has a data rate of 100 bps. The modem parses message data into 9 bit packets, which are comprised of 8 data bits and 1 stop bit. There is no parity bit included in the packet. The transmitted message can vary in length from 1 to 144 bytes. Figure 3.3 shows the format of the Aero-Astro data packet.

Preamble (1 byte)	Length (1 byte)	Command (1 byte)	Data (message)	CRC (2 bytes)

Figure 3.3. Aero-Astro Simplex Modem Data Packet (From Figure 11 of [24], © AEROASTRO. Reproduced with permission.)

Axonn's AXTracker integrates the Aero-Astro simplex modem with a GPS engine. This integration allows the modem to transmit its GPS position at a programmed interval. The AXTracker has an internal antenna and an external power source. Axonn provides *geofencing* capabilities and online data access for their customers. Geofencing allows a user to define a specific, closed geographical area in the modem. If the modem senses that it moves across the line (the *fence*) specified by the user, it transmits an alarm. While the AXTracker shares many of the same technical specifications of the Aero-Astro modem, its dimensions are much larger at 9.25" X 6.25" X 1". These dimensions are much larger than the desired device dimensions.

3.2 Communications Link

The Globalstar communications link is based on a code-division multiple access (CDMA) waveform. The communications link will be presented in the terminology defined in the Overview: Forward Link and Reverse Link. The other important characteristics of the Globalstar System are the power management scheme and soft hand-offs. Table 3.3 shows the reverse link uplink power budget, and Table 3.4 shows the reverse link downlink power budget.

The Globalstar System uses a total RF bandwidth of 16.5 MHz, which is frequency-divided into 13 channels, each 1.23 MHz wide. The multipath losses in the Globalstar system can be approximated by a Rician distribution because a line-of-sight (LOS) component plus signals degraded by multipath are present at the receiver [15,57]. The minimum link propagation delay is 9.4 ms at a satellite elevation of 90˚, and the maximum link propagation delay is 23.4 ms at a satellite elevation of 10˚ [46]. In this context, propagation delay is defined as the time delay between the data transmission by the user device and the data reception at the gateway. The propagation delay varies with satellite elevation because the path length between the satellite and user changes with elevation. At azimuth, the path length is the shortest (1414 km, in this case), and the path length is longest when the satellite is on the horizon (3510 km here). Propagation delay can be calculated by dividing the distance traveled by the speed of light, so a longer path length corresponds to a longer propagation delay.

3.2.1 The Forward Link

The Forward Link in the Globalstar system describes communications from the gateway to the satellite to the user device. The uplink frequency range is 5091 - 5250 MHz (C Band), and the downlink frequency range is 2483.4 - 2500 MHz (S Band) [11,40,46]. In addition to the CDMA waveform, the data is processed using a pseudo-random (PN) binary orthogonal code. This binary code provides isolation between the signals transmitted by the gateway and creates unique signals for each beam, satellite, and gateway. These provisions prevent the Globalstar system from interfering with itself because of the properties inherent in CDMA systems. Since DS-SS signals are transmitted as such low power levels, many signals can be present in the same

bandwidth without causing destructive interference. These properties allow a large number of simultaneous links within a single channel. DS-SS and CDMA are discussed in more detail in Chapter 4.

Convolutional encoding with interleaving is used as a method of Forward Error Correction (FEC) to decrease the number of errors at the receiving end of the link. FEC decreases the bit error rate by both spreading out and randomizing the data to protect against channel errors – and burst errors in particular. FEC is discussed in more detail in Chapter 4. Finally, the channel is scrambled to ensure privacy in the link [40].

3.2.2 The Reverse Link

The Reverse Link in the Globalstar system describes communications from the user device to the satellite to the gateway. The uplink frequency range is 1610-1626.5 MHz (L Band), and the downlink frequency range is 6875-7055 MHz (C band) [11,40,46]. The reverse link waveform is very similar to the forward link waveform with the following differences. A fixed time offset is added to the PN code to create a unique signal for each user device. This unique signal allows the gateway to properly identify each user device and also provides user privacy and system capacity through a large possible address space. Instead of the binary code used in the forward link, the reverse link utilizes a 64-ary orthogonal code to simplify demodulator implementation [40].

3.2.2.1 Reverse Link Budgets

Table 3.4 shows the uplink power budget for the Reverse link, which describes the power and noise levels on the link between the user and the satellite transponder. This link budget only applies for a single user accessing the transponder. After the link budgets are presented, a discussion of the additional losses from other users is presented.

Several parameters must be defined in order to complete the link budget. For these calculations, the value used for the speed of light (c) was 299792500 m/s, and the value used for

the radius of the earth (r_e) was 6378 km. The wavelength (λ) was calculated to be 0.186 m using Equation 3.1.

$$\lambda = \frac{c}{f} \tag{3.1}$$

Typically, Equation 3.2 is used to calculate the gain (G) of an antenna. In Equation 3.2, A_e is the effective area of the antenna, and is determined by multiplying the physical area of the antenna by an efficiency factor. However, the efficiency of the satellite antennas was unknown, so the gain of the antennas was approximated by Equation 3.3 [45].

$$G = \frac{4\pi A_e}{\lambda^2} \tag{3.2}$$

$$G \approx 10 \log\left(\frac{33{,}000}{\Theta_w \Theta_h}\right) \tag{3.3 [45]}$$

In Equation 3.3, Θ_w and Θ_h represent the horizontal and vertical beamwidths of the satellite beam and are used to approximate the gain of the satellite receive and transmit antennas. These values were measured from Figure 3.4 for an edge beam; the values for an edge beam were used for a worst case approximation. The beam outlined in the dashed line was used for the gain calculation.

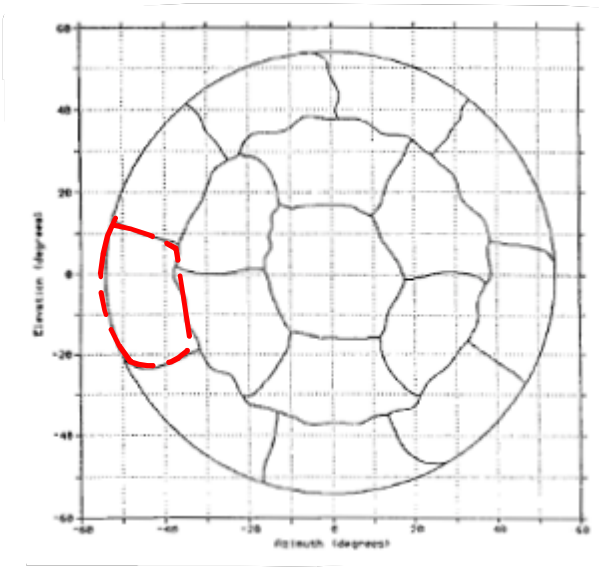

Figure 3.4. Beam pattern for a Globalstar System satellite beam (footprint) © [1998] IEEE. Reprinted, with permission, from [11]

Using Figure 3.4, the center beam was measured having a beamwidth of 25˚ and a beam height of 32˚, and the (outlined) edge beam was measured having a beamwidth of 18˚ and a beam height of 30˚. Using the beamwidths for the edge beam in Equation 3.3, the gain of the satellite receive antenna (G_r) was calculated to be 17.9 dB. This value is 1.7 dB higher than the approximate gain for a center beam. This difference makes sense because many satellite system service providers increase the effective gain of the outer beams to help combat edge of beam loss. In spite of these calculations, [23] gives the uplink antenna gain as 31.8 dB, which is significantly higher than the gain calculated from Equation 3.3. The antenna gain given in [23] was used in the link budget calculation because the transponder receive antenna may have additional gains not accounted for in Equation 3.3.

The maximum path length between the user and the satellite is when the satellite is on the horizon. Using the law of sines, the maximum path length (R) was calculated at 4482.5 km. Using this path length, the path loss (L_p) was calculated to be 169.6 dB using Equation 3.4.

$$L_p = 20\log\left(\frac{4\pi R}{\lambda}\right) \qquad 3.4$$

The values assumed for the remaining link budget calculations are summarized in Table 3.3

Parameter	Assumed Value
Noise Temperature at satellite transponder	550 K
Noise Bandwidth of receiver	1.23 MHz
User Transmit Power	0.75 W
User Transmit Antenna Gain	0 dB

Table 3.3. Assumed parameter values for the uplink budget calculation. For the simulation in Chapters 5 and 6, the user transmit power was varied over the range 50 mW to 2 W.

For this link budget and for the downlink budget, a user transmit power of 0.75 W was assumed. However, for the single user simulation, the user transmit power was tested at 0.25, 0.5, 0.75, 1, and 2 W. For the multiple user simulation, the beacon transmit power was varied between 50 mW and 2 W, depending on the loading of the system. The additional losses (1 dB) in the received power calculation account for atmospheric losses and antenna polarization losses. The beam-edge loss (3 dB) in the same calculation accounts for the loss in signal power at the

edge of the satellite footprint. It is common in a satellite system for the power level to degrade a few decibels at the edge of a footprint; the beam-edge loss takes this effect into account.

Reverse Uplink (User to Satellite):

Frequency	1610 – 1626.5 MHz
Path Length (R)	4482.5 km
Wavelength (λ)	0.186 m
Path Loss (L_p)	**169.6 dB**
Boltzman's Constant (k)	-228.6 dBW/K/Hz
Noise Temperature (T)	27.4 dBK
Noise Bandwidth (B)	60.9 dBHz
Noise Power (N)	**-140.3 dBW**
Transmit Power (P_t)	-1.2 dBW
Transmit Antenna Gain (G_t)	0 dB
Receive Antenna Gain (G_r)	31.8 dB
Path Loss (L_p)	-169.6 dB
Additional Losses	-1 dB
Beam-edge Loss (L_{eob})	-3 dB
Received Power (P_r)	**-143 dBW**
Carrier-to-Noise Ratio (C/N)	**-2.7 dB**

Table 3.4. Reverse Link, Uplink Power Budget (single user)

Table 3.6 shows the calculation of the downlink power budget for one user on the reverse link. Recall that the reverse downlink describes the communication from the satellite to the gateway. Where applicable, values calculated for the uplink were used. Values for the power level and gain of the satellite transponder are from [23]. The total power available to a Globalstar satellite transponder is 1000 W. However, this power must be divided between all users in all of the beams (16 beams). It is not known how the satellite divides the power between its transponders, and the amplification levels at the satellite transponder are not clearly stated; however, [23] gives a downlink EIRP of –1.5 dBW. This value was used for the single user link budget of Table 3.6. Another method of determining satellite output power was used for the multiple user case, which is described below.

Parameter	Assumed Value
Noise Temperature at the receiver	120 K
Noise Bandwidth at the receiver	1.228 MHz
Satellite Transmit EIRP	-1.5 dB
Gateway Receive Antenna Gain	50 dB

Table 3.5 Assumed parameter values for downlink budget calculation.

The gain of the satellite transmit antenna is assumed to be the same as in the uplink budget calculation (17.9 dB), and the maximum path length (4482.5 km) is also assumed to be the same. For this calculation, the receiver is operating in clear air conditions (no rain). Using Equation 3.1, the wavelength for the downlink was calculated at 0.0436 m, resulting in a path loss of 182.2 dB. The transmit power from the satellite transponder was calculated from the sum of the satellite repeater gain and the power received at the satellite transponder. An additional 3 dB must be subtracted to account for transponder back-off. Even though the satellite transponder is linear (or bent-pipe), it cannot be operated at full power or it will saturate. Back-off prevents the power level in the transponder from approaching the saturation level.

Reverse Downlink (Satellite to Ground station)

Frequency	6875 – 7055 MHz
Path Length (R)	4482.5 km
Wavelength (λ)	0.0436 m
Path Loss (L_p)	**182.2 dB**
Boltzman's Constant (k)	-228.6 dBW/K/Hz
Noise Temperature (T)	20.9 dBK
Noise Bandwidth (B)	60.9 dBHz
Noise Power (N)	**-146.8 dBW**
Transmit EIRP	-1.5 dBW
Receive Antenna Gain (G_r)	50 dB
Backoff	-3 dB
Path Loss (L_p)	-182.2 dB
Additional Losses	-1 dB
Beam-edge Loss (L_{eob})	-3 dB
Received Power (P_r)	**-140.7 dBW**
Carrier-to-Noise Ratio (C/N)	**6.1 dB**

Table 3.6. Reverse Link Downlink Power Budget (single user)

Both link budgets include an allowance – or margin – for edge of beam loss. Even though the margin is 3 dB, this is considered the worst-case performance in a particular beam. As the elevation of the satellite increases, the beam edge loss decreases. Performance will only improve will high elevation angles. These link budgets assume worst-case scenario parameters to ensure system operation. An optimization could be performed to determine the average required link margin, but this optimization is not calculated here.

Even though the downlink power budget shows a C/N ratio of 6.1 dB, the uplink C/N ratio must be taken into account when determining the overall C/N ratio seen by the receiver. Using the reciprocal formula of Equation 3.5 [45].

$$\frac{1}{(C/N)_o} = \frac{1}{(C/N)_{up}} + \frac{1}{(C/N)_{dn}} \qquad 3.5$$

Note that the C/N values in Equation 3.5 must be in ratio format, not decibel format. The overall C/N ratio at the receiver is –3.2 dB. This link is limited by the uplink carrier-to-noise ratio, as expected.

3.2.2.2. Multiple Access Interference

In CDMA systems, transmissions from one user will interfere with the other users' transmission. This interference results from both a decrease in the C/N ratio and from varying user transmit power levels. The decrease in the C/N ratio is cause by an increased amount of interference (*I*) from other users. System performance will be degraded if the user transmit power levels are not equal; this effect is referred to as the *near-far* effect and is discussed in detail in Section 3.2.3.

The amount of interference is proportional to the number of users in the system that are accessing the satellite transponder at the same time. This type of interference is typically treated as noise. Because of this treatment, the interference power level can be added to the noise power level. Equation 3.6 [45] describes the relationship at the receiver between the noise, interference, and the number of users:

$$\frac{C}{N+I} = 10\log\left(\frac{C}{N_t + C(Q-1)}\right) \qquad 3.6\ [45]$$

where C is the received power level of one signal, N_t is the thermal noise power, and Q is the total number of signals present in the receiver, and all power levels are in Watts. The multiple access interference is $C(Q-1)$; it is intuitive that for only one user, the C/N ratio is calculated as shown in Tables 3.5 and 3.6.

For the multiple access interference cases considered in Chapters 5 and 6, three different levels of system loading were considered; C/(N+I) ratios were calculated for various transmitter power levels in each multiple user case considered. Section 5.2 discusses these cases in detail.

3.2.3 Power Management

In order to achieve maximum capacity in a CDMA system, the received signal-to-noise ratio must be the same at the gateway for all user devices. If one received signal is larger than the others at the gateway, that signal will interfere with the other signals, reducing system performance and capacity. If one user terminal is much closer to the receiver than other terminals, the signal from that terminal will appear larger than the signals from the other terminals. The large signal will introduce a large amount of interference to the other signals at the receiver. This effect is called the *near-far effect*, and is common in cellular and other mobile systems. Globalstar deals with this problem though power management techniques [15,40].

To maximize system capacity, the Globalstar system incorporates power management schemes in both its Forward and Reverse communication links. On the Reverse link, the gateway measures the received power level of a user terminal and compares it to a threshold. The gateway can then issue a command over the control channel to the user terminal to either increase or decrease its transmit power, depending on the results of the power measurement. On the Forward link, power management is implemented at the gateway through power level measurements received from the user terminal. The user terminal periodically measures the strength of the signal it is receiving and transmits this information back to the gateway. If the received power measured by the user terminal is less than the minimum required power, a message is immediately sent to the gateway. Upon receiving this message, the gateway can increase its transmit power or redistribute power from other user terminals to improve link quality [40,46].

3.2.4 Soft Handoffs

In a typical LEO satellite communication system, when the satellite being used to create the link moves out of view, the link is lost, and a new link must be established with another

satellite. Since Globalstar satellites are only in view between 10-15 minutes, this system of establishing links would be very cumbersome. To prevent this encumbrance, the Globalstar system was designed to accommodate soft handoffs [15,20,40]. As mentioned in the Section 3.1, the Globalstar satellite constellation was designed so that at least two satellites (with a minimum elevation of 10˚) would be in view from any service location at all times. A possible scenario is depicted in Figure 3.5. When both satellites are in view, the gateway arranges for a beam from each satellite to be used in the link. When one satellite (A) moves out of view, the link is completely transferred to the remaining satellite (B). When the next satellite (C) comes into view, the gateway will again arrange for a beam from each satellite (now B and C) to be used in the link. This capability allows a link to exist for (theoretically) as long as the user needs it. Soft handoffs are accomplished by implementing rake receivers in the user terminals. Rake receivers allow a single receiver to constructively combine multiple signals arriving at different times if the time difference of arrival is greater than one chip, which is the case in soft handoffs. Rake receivers are discussed in more detail in Section 4.2.1.

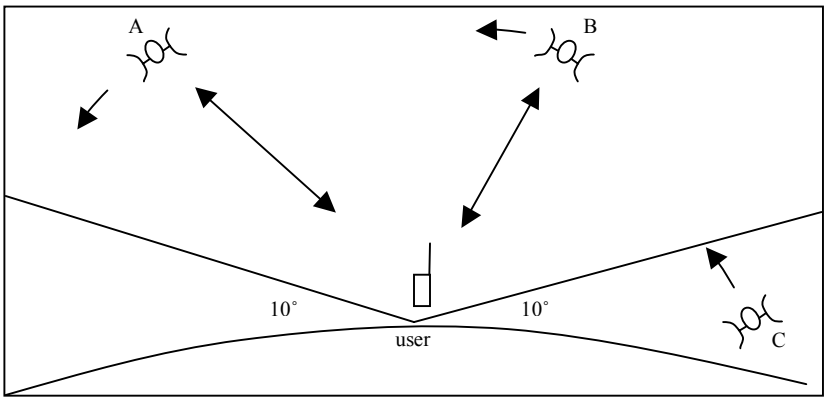

Figure 3.5. Globalstar Soft handoff scenario

Chapter 4

Technical Background

The Globalstar Satellite System uses Code Division Multiple Access (CDMA) to allow many sources to transmit data through the satellite transponders simultaneously. The operating principles of the Globalstar system were adapted from those defined in the IS-95 standard. A brief overview of the IS-95 standard is provided, as well as a description of the changes made to implement the standard in a satellite communication system.

Because Globalstar is a satellite communication system with a low carrier-to-noise ratio at the satellite transponder, some form of error correction should be implemented. According to [8,10,40] the Globalstar System utilizes convolutional encoding for error correction. Turbo coding might provide better performance, but the packet size may be too small to obtain the performance benefit. Turbo coding is a variant of convolutional coding that provides much better performance than standard convolutional coding. This chapter gives an overview of both DS-SS communications and error correction codes.

The Global Positioning System (GPS) and the Globalstar system share several design characteristics and challenges. The most significant similarity is the challenge of correctly receiving a Doppler-shifted DS-SS signal. The GPS solution to this problem will be described, along with its relevance to the design of the Globalstar receiver.

4.1 Direct Sequence Spread Spectrum (DS-SS)

Direct Sequence Spread Spectrum (DS-SS) is a technique in which a narrowband data signal is multiplied by a long binary sequence, called a spreading waveform (or chip sequence). This multiplication results in a high data rate and, therefore, a wide bandwidth for the transmitted data. At the receiver, the incoming signal is multiplied again by the spreading sequence, which – when properly aligned – effectively removes the spreading sequence and recovers the original narrowband data. Figure 4.1 shows a narrowband data signal before (solid line) and after spreading (shaded area).

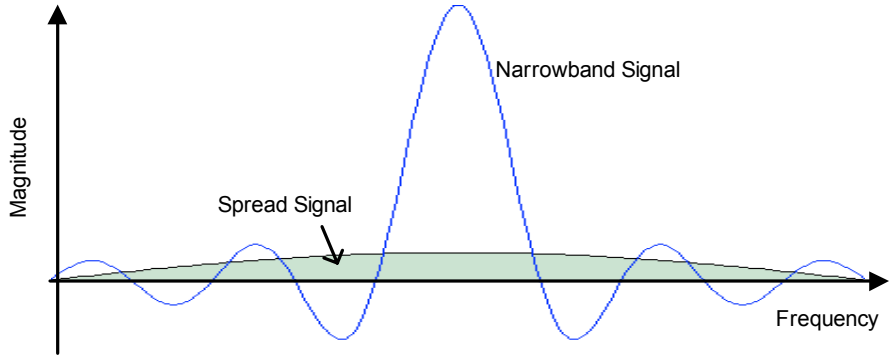

Figure 4.1 Direct Sequence – Spread Spectrum Waveform (spread signal). The Narrowband data represents the signal before spreading.

In Figure 4.1, the first nulls of the narrowband signal occur at $\pm 1/T$, and the first nulls of the spread signal occur at $\pm 1/T_c$, where $1/T$ is the bit rate of the narrowband signal, and $f_c = 1/T_c$ is the chip rate of the spreading sequence.

The Globalstar satellite system uses DS-SS to implement Code Division Multiple Access (CDMA) for two primary reasons. The first is that DS-SS transmitters are simpler in design than those required for Time Division Multiple Access (TDMA) or Frequency Division Multiple Access (FDMA). In FDMA systems, both the transmitters and receivers must have very accurate center frequencies, and the ground station (or base station) must have a separate receiver for each carrier frequency in order to receive those carriers. These requirements translate into complex devices. In TDMA, the transmitter (user device) must have very accurate

timing and fast synchronization circuits. In order to receive a signal, the receiver must achieve frame synchronization within a few microseconds and bit synchronization immediately after. These requirements lead to high cost and very complex systems [45].

The second reason for using CDMA (DS-SS) is that DS-SS allows signals from two satellites or two satellite beams to overlap without significant interference. Note that CDMA (DS-SS) allows signals to overlap more than the overlap in FDMA or TDMA systems.

4.1.1 Spreading Sequences

A DS-SS signal is the product of a narrowband data sequence and a spreading sequence. To create the benefits of spread spectrum communication listed above, spreading sequences must have several important properties:

1. Be easy to generate,
2. Behave like noise (statistically), and
3. Be sufficiently long.

A spreading sequence must be easy to generate to facilitate system design. The sequence must be long to provide the required processing gain, and the sequence must behave like noise for proper signal recovery at the receiver.

Because there are different applications of spread spectrum communication systems, there are two types of spreading sequences – pseudo-random noise (PN) and orthogonal – to accommodate different applications. PN sequences are used in systems that require protection from jamming or low probability of interception by using long sequences. Orthogonal sequences are generally used for multiple access systems or for multiplexing data, but are generally shorter than PN-sequences. PN-sequences are more commonly used than orthogonal waveforms because the latter requires time synchronization and has poor auto-correlation properties.

4.1.1.1 Correlation

In a spread spectrum system, data is extracted from the receiver by multiplying the incoming signal by the spreading sequence. In order to properly extract the data, the spreading

sequence must have specific, predictable behavior when it is multiplied by itself or a time-shifted version of itself. These properties are defined below in Equations 4.2 and 4.4.

Auto-correlation – the result of multiplying a signal by itself – is defined as

$$C_{jj}(n) = \frac{1}{N}\sum_{i=0}^{N-1} a_{j,i} \cdot a_{j,i+n} \tag{4.1}$$

where N is the length of the spreading sequence and $a_{j,i}$ is the ith value of the jth spreading code. Ideally, we want the auto-correlation to equal one when the signal is multiplied by itself (meaning it is properly aligned) and zero otherwise, as shown in Equation 4.2.

$$C_{jj}(n) = \begin{matrix} 1, & n = 0 \\ 0, & n \neq 0 \end{matrix} \tag{4.2}$$

Cross-correlation – the result of multiplying one signal by another signal – is defined as

$$C_{jk}(n) = \frac{1}{N}\sum_{i=0}^{N-1} a_{j,i} \cdot a_{k,i+n} \tag{4.3}$$

where N is the length of the spreading sequence, $a_{j,i}$ is the ith value of the jth spreading code, and $a_{k,i+n}$ is the ith value of the kth spreading code. Ideally, $C_{jk}(n)$ will equal zero when j is not equal to k for all values of n, as shown in Equation 4.4.

$$C_{jk}(n) = 0, \quad \forall n,\ j \neq k \tag{4.4}$$

The codes used in the simulation presented in Chapters 5 and 6 approach this definition of ideal performance when properly aligned.

4.1.1.2 PN Sequences

A PN sequence is a long data sequence with statistical characteristics similar to additive white Gaussian noise (AWGN). Specifically, PN-sequences have cross-correlation values near zero and near auto-correlation performance (as defined in Equation 4.2). There are several types of PN-codes commonly used in CDMA systems: Maximal length (m-sequences), Gold Codes, and Kasami Sequences. Only m-sequences and Gold Codes will be discussed in this paper.

Maximal length sequences (or m-sequences) are generated by a feedback shift register. The modular (or parallel) block diagram for generating m-sequences is shown in Figure 4.2.

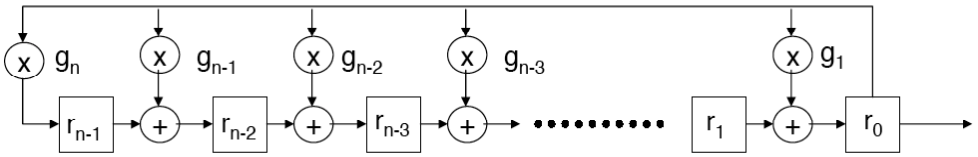

Figure 4.2. Modular Format of Feedback Shift Register for generating m-sequences. The initialization vector is represented by r_{n-1}, …, r_0, and the coefficients of the generator polynomial are denoted by g_n, …, g_1. (Reproduced from [6] with permission.)

The initial state of the register – also called the initialization vector – is represented by r, the feedback taps are represented by g, and n is the number of registers (and the degree of the sequence). The length (L) of the m-sequence is determined by the number of shift registers, where

$$L = 2^n - 1. \tag{4.5}$$

The initial state of the register is arbitrary, but cannot be all ones. There are many published tables defining feedback tap values.

In general, m-sequences are used to create spread spectrum signals because of their auto-correlation properties. Theoretically, for an m-sequence of length L, the autocorrelation has the values

$$C_{jj}(n) = \begin{cases} 1, & n = 0, L, 2L, \ldots \\ -\dfrac{1}{L}, & otherwise \end{cases} \tag{4.6}$$

using the definition of autocorrelation given in Equation 4.1. In practice, noise may cause the autocorrelation to be larger than the values giving in Equation 4.6, particularly in the case where n is not an integer multiple of L.

Although m-sequences have excellent auto-correlation properties, they do not have good cross-correlation properties. Another problem with m-sequences is there are not many sequences. For applications where many codes are needed, Gold codes should be used. There are many other important properties of m-sequences, which can be found in literature [13,30,43].

Gold codes result from the modulo-2 sum of a preferred pair of m-sequences. A preferred pair of m-sequences is defined by their cross-correlation:

$$C_{jk}(m) \in \quad -\frac{1}{L}\left(1+2^{(n+1)/2}\right), -\frac{1}{L}, \frac{1}{L}\left(2^{(n+1)/2}-1\right) \quad , \quad n \text{ odd} \tag{4.7}$$

$$C_{jk}(m) \in \quad -\frac{1}{L}\left(1+2^{(n+2)/2}\right), -\frac{1}{L}, \frac{1}{L}\left(2^{(n+2)/2}-1\right) \quad , \quad n \text{ even} \tag{4.8}$$

The most important result of these cross-correlations is that the values are bounded. In multiple access systems, interference is proportional to the value of the cross-correlation of the codes at the receiver. Since there is a high potential for many codes to arrive at the receiver at the same time, it is important that they all have low cross-correlation values.

A block diagram for generating Gold codes is shown below in Figure 4.3. Although Gold codes are the modulo-2 sum of preferred pairs, additional Gold codes can be generated by simply changing the initial state of one of the registers.

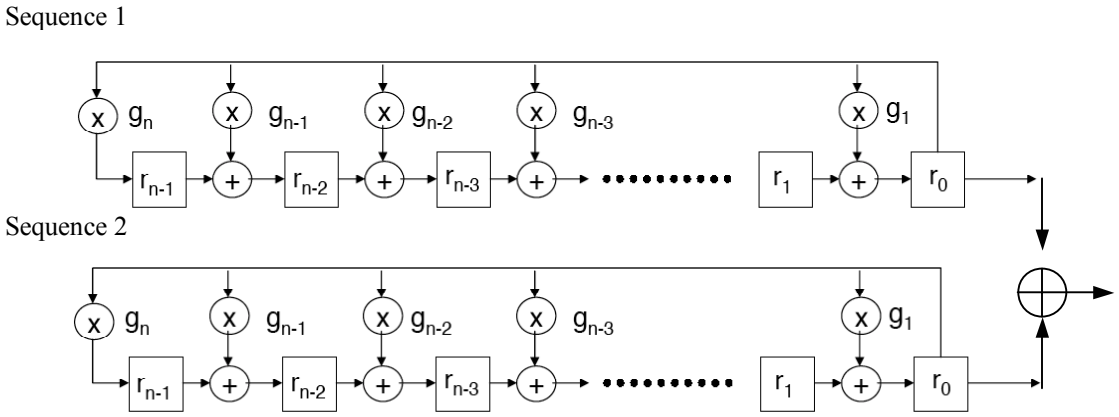

Figure 4.3. Gold Sequence Generator. The initialization vector is represented by r_{n-1}, …, r_0, and the coefficients of the generator polynomial are denoted by g_n, …, g_1. (Reproduced from [6] with permission.)

4.1.1.3 Orthogonal Codes

Orthogonal waveforms (also called Walsh Codes) provide short spreading codes for multiple access communication systems, where it is desirable for each signal arriving at the receiver to be uncorrelated to any other signal arriving at the receiver. This type of signal attribute reduces interference and results in higher signal-to-noise ratio (SNR). The defining

property of a Walsh Code is that all the codes in a set are orthogonal. For a set of K Walsh codes of length K, orthogonality over period T, is defined as:

$$\int_0^T w_n(t)w_m(t)dt = \begin{cases} K, & n = m \\ 0, & n \neq m \end{cases} \qquad 4.9\ [22]$$

This relationship is similar to Equation 4.3 – cross-correlation, so it can be said that Walsh Codes have good cross-correlation properties. However, Equation 4.9 only applies if $w_n(t)$ and $w_m(t)$ are synchronized in time. The length, K, of a Walsh sequence is limited to

$$K = 2^n \qquad 4.10$$

where n is an integer. A Walsh sequence can be created by re-ordering high order Hadamard matrices. A Hadamard matrix is a square matrix whose values are in the set [-1,1]. By definition, a Hadamard matrix of order n, where $n = 2^m$, must have $n(n-1)/2$ negative ones and $n(n+1)/2$ positive ones. This property is similar to one of the properties of m-sequences. The first Hadamard matrix ($m = 1$) is defined as:

$$H_2 = \begin{matrix} 1 & 1 \\ 1 & -1 \end{matrix} \quad \text{or} \quad \begin{matrix} 1 & 1 \\ -1 & 1 \end{matrix} \qquad 4.11$$

High order Hadamard matrices are generated by the equation:

$$H_K = H_{K/2} \otimes H_2 \qquad 4.12\ [21]$$

Walsh sequences of length K are created from the rows of matrix H_K such that transitions from positive to negative one occur only at fixed intervals.

The cross-correlation properties of Walsh codes depend not only on sequence time synchronization, but also on an AWGN channel (i.e. no multipath). Because of the limitations of Walsh Codes, they are often used in conjunction with PN-sequences, referred to as layered spreading codes. Layered spreading codes are often used when the auto-correlation properties of PN-sequences are needed, but the cross-correlation properties of orthogonal codes are also desired.

4.1.2 DS-SS in the Globalstar Satellite System

Different coding schemes are employed in the Globalstar Satellite System to accommodate the different requirements for the forward and reverse links. Globalstar utilizes a variation of the IS-95 CDMA cellular standard. The IS-95 standard introduced the Rake receiver to increase diversity in a multipath fading environment and also to implement soft handoffs. The Globalstar system utilizes both of these advantages to improve system performance.

4.1.2.1 The Forward Link

In the Forward Link, two PN sequences are generated to implement quadraphase PN modulation, where each sequence is of length $2^{17} - 1$. These PN sequences are used to differentiate between satellites, beams, and gateways. A gateway transmits one PN sequence, but changes the time offset for each beam of each satellite in view. The gateway signal is layered with a Walsh code of length 128. These channels are divided into 119 traffic channels, 7 paging channels, 1 pilot channel, and 1 synchronization channel [40]. The use of Orthogonal codes for channel definition increases the correlator output, maximizing the cross-correlation value. The gateway assigns a specific traffic channel (Walsh code) to a user terminal via the synchronization channel.

4.1.2.2 The Reverse Link

The Reverse Link is more complex than the Forward Link in that it utilizes two PN sequences of different length. The first PN sequence is the same as used in the Forward Link, of length $2^{17} - 1$. The second PN sequence is much longer ($2^{42} - 1$) and is used to identify user terminals at the gateway. The time offset for the second sequence is determined by the user terminal address, uniquely identifying each terminal to the gateway. This long PN sequence allows for a large number of users and a high level of security. As in the Forward Link, the combined PN sequences are layered with a Walsh code, but with length 64 for the Reverse Link. While on the Forward Link the Walsh code is set by the gateway, the data being transmitted determines which Walsh code will be used. Using the data to select a Walsh code enables faster demodulation of data at the gateway.

This simulation presented in this thesis is based on the reverse link. Link budgets for the reverse uplink and downlink are presented in Section 3.2.2.

4.1.3 Receiving DS-SS

A block diagram of a generic spread spectrum receiver is shown in Figure 4.4. In the correlator, the correlation properties of PN sequences become crucial to correct operation.

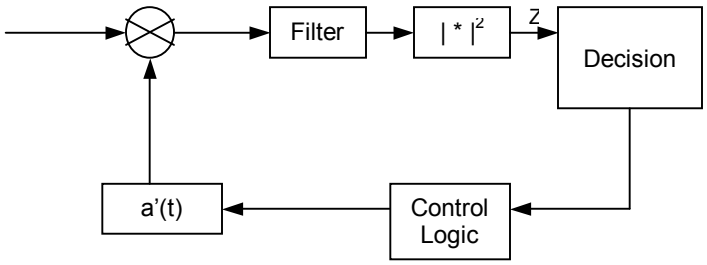

Figure 4.4 Spread Spectrum Receiver Block Diagram (Reproduced from [6] with permission.)

If we model the transmitted spread signal as

$$s(t) = \sqrt{2P}a(t)b(t)\cos(2\pi f_c t + \Theta) \qquad 4.13\ [22]$$

where P is the signal power, $a(t)$ is the spreading waveform, and $b(t)$ is the data, f_c is the carrier frequency, and Θ is the carrier phase, then we can model the received signal as

$$r(t) = \sqrt{2P}a(t-\tau)b(t-\tau)\cos(2\pi(f_c - f_d)t + \Theta) + n(t) \qquad 4.14\ [22]$$

where τ is the time delay of the received signal, f_d is the frequency offset of the signal, Θ is the carrier phase plus some error, and $n(t)$ is the noise from the channel. The time delay, τ, is influenced by the propagation delay of the signal. The frequency offset, f_d, is influenced by the velocity of the satellite or the receiver. We will assume the phase error, Θ, to be negligible and able to be corrected during demodulation. In addition, both f_d and τ are affected by the channel noise $n(t)$.

In satellite systems, the frequency offset is often the Doppler frequency, f_d, resulting from the motion of the satellite relative to the receiver. In the system modeled in this thesis, the

receiver is stationary, but the transmitter is mobile. Because the position of the receiver relative to the satellite can easily be calculated – and therefore, the Doppler shift can be calculated – the Doppler shift caused by the velocity of the satellite relative to the receiver can be removed. In the case of the transmitter, its position relative to the satellite is unknown until after the message is received, so the Doppler frequency cannot be directly calculated as in the case of the receiver. Doppler frequency can be defined as

$$f_d = \frac{v}{\lambda}\cos\varphi \qquad 4.15$$

where v is the velocity of the satellite, λ is the wavelength of the transmitted signal, and φ is the angle between the satellite velocity vector and the receiver position vector. When v is the maximum velocity, the resulting Doppler frequency is the maximum Doppler shift, but must be applied in both positive and negative directions.

When the signal is received, it first enters the correlator. However, the receiver does not know the actual time or frequency shift of the incoming signal. The receiver starts correlating the signal with an estimated time- and frequency-shifted version of the spreading code. The time shift estimate is denoted $\hat{\tau}$, and the frequency shift estimate is denoted $\hat{f}$. The time and frequency shifts will be incremented over all possible values until the correlator returns a match. Equation 4.16 shows the correlation equation;

$$Z = r(t-\tau)a(t-\hat{\tau})\cos(2\pi(f_c - \hat{f}_d)t + \Theta) + n(t) \qquad 4.16$$

the operation of the receiver is discussed in greater detail in Chapter 5, including discussions on search strategies and decision strategies.

4.2 Cellular Standard IS-95A

Interim Standard 95 (IS-95) was introduced by the Telecommunications Industry Association in 1993. The standard specifies the attributes for CDMA cellular systems, including frequency allocation, data rates, power control, hand-offs, and registration. The standard also

provides guidance for interfacing with the switched public telephone network. The Globalstar Satellite Communication System was derived from the IS-95 specification. Table 4.1 compares the IS-95 system parameters with the Globalstar system parameters.

Parameter	IS-95	Globalstar
Multiple Access Method	CDMA/FDM	CDMA/FDM
Channel Spacing	1.25 MHz	1.23 MHz
Chip Rate	1.228 Mbps	1.228 Mbps
Data Modulation	BPSK	BPSK
Layered Spreading Code		
Walsh Code length	64	128 (Forward link) 64 (Reverse link)
PN-sequence degree	15	17 (Forward link) 17, 42 (Reverse link)
Data rate	4.8 or 9.6 kbps	4.8 kbps

Table 4.1. Comparison of IS-95 and Globalstar System Parameters

The IS-95 standard sets up the channel architecture used by Globalstar: 1 pilot channel, 1 synchronization channel, paging channels, and traffic channels. Paging channels are used by the gateway to transmit control information to user terminals, such as power control commands. The IS-95 standard allocates seven paging channels and the Globalstar system utilizes all seven channels. The IS-95 standard also introduced the implementation of a Rake receiver to combat multipath degradation and implement soft handoffs.

4.2.1 Rake Receiver

The concept of a Rake receiver was first introduced by Price and Green in 1958. A Rake receiver utilizes several *fingers* to constructively combine multipath components. Each finger of a Rake receiver is a correlator with a different phase offset. The number of fingers corresponds to the number of phase offsets the receiver can decorrelate in parallel. The output from each finger is combined to create a final decision in the receiver and locate the transmitted signal. Before combining, the output of each finger is weighted to improve the overall decision value [13,22,30].

There are many methods of combining the outputs of each correlator; three methods are discussed here. One method is *Equal Gain Combining*, and assigns an equal weight to each correlator output before combining them. The drawback of this method is that a noisy path will still significantly degrade the performance of the decision device by lowering the overall correlator output. Another method is *Selection Combining*, in which only the largest output from all the fingers is used to determine the code position. The benefit of this method is that noisy signals are discarded; however, this method does not use all of the available energy in the receiver. The third method is *Maximal Ratio Combining*. This method uses an algorithm to set the weights for each finger such that when the fingers are combined, the resulting signal-to-noise ratio is maximized. Maximal Ratio Combining is the most often implemented combining method in Rake receivers because it provides the best performance of the combination methods presented here.

One environment in which Rake receivers are particularly helpful is a multipath fading environment. In a multipath fading environment, each fade occurs independently. Using this knowledge, it is unlikely that more than one signal will suffer from a large fade. The Rake receiver exploits this fact by utilizing the signal component least affected by fading. In order to successfully combine multipath components, the time delay between the arrival of the signals must be larger than one chip [13,22,30].

4.2.2 Diversity in the Globalstar Satellite System

Diversity in a communication system refers to methods or techniques for improving reception performance. There are four types of diversity in communication systems: space diversity, frequency diversity, time diversity, and phase diversity.

The Rake receiver discussed above exploits phase diversity to improve the performance of the receiver. As shown by the Rake receiver, designing a receiver to collect a transmitted signal at several different phase offsets and then constructively combining those signals significantly improves reception performance in a noisy environment, particularly when multipath fading is present. Another method of providing phase diversity is by using antennas with different polarizations to receive a signal. With this method, the signal can be received regardless of its polarization. Looking at the operation of the Rake receiver in time rather than

frequency, the Rake receiver provides time diversity by combing versions of the transmitted signal arriving at the receiver at different times.

Frequency diversity is achieved by transmitting a signal on several carrier frequencies and constructively combining the signals at the receiver. Space diversity is achieved in a wireless system by utilizing several receivers at different locations. This type of diversity is often utilized in cellular systems, where a base station may have two receive antennas, each with a different orientation. The receiver will utilize the antenna receiving the stronger signal. This type of diversity is also referred to as antenna diversity because more than one antenna is used to improve the performance of the receiver.

The Globalstar Satellite System uses a Rake receiver to achieve phase diversity to improve performance in the multipath environment. As described above, the multipath components must be separated in time (or distance) by more than one chip. In the Globalstar system, this corresponds to 0.8 μs or 250 m. If the separation between multipath components is less than 0.8 μs in time or 250 m in space, the Rake receiver will not provide much benefit. To prevent this situation from occurring, overlapping beams (from one or more satellites) are used to create *artificial multipath* [40]. For more information on the implementation of Rake receivers in the Globalstar Satellite System, the reader is referred to [5,20,35].

4.3 Channel Coding

Channel coding, sometimes referred to as Error Control Coding provides protection against bit errors in wireless communication systems. There are two parts to error control: detection and correction. Error detection is the ability of a system to detect errors in a received data stream due to channel interference. Error correction is the ability of a system to correct errors in a received data stream due to channel interference. There are two classes of channel coding for error detection *and* correction: Automatic Repeat Request (ARQ) and Forward Error Correction (FEC). ARQ techniques become impractical for systems with long transmission delays, such as satellite communication systems; therefore, we will focus on FEC coding.

4.3.1 The Shannon Limit

Shannon's Coding Theorem states that for a given communications channel with capacity, *C*, the maximum rate of transmission, *R*, which guarantees the minimum probability of error at the receiver exists such that $R < C$. The minimum probability of error cannot be achieved without coding, so the Coding Theorem implies there must be some method of coding which achieves the minimum probability of error for data transmission in a channel. Theoretically, the Coding Theorem states that it is possible to transmit data without error at a rate less than *C*.

The Shannon Limit, also known as the Shannon-Hartley Theorem, establishes the channel capacity, *C*, for an AWGN channel, from which follows the maximum rate of transmission, *R*, in *C*:

$$R_{\max} = B\log_2\left(1+\frac{S}{N}\right) \ bits/s \qquad 4.17\ [22]$$

where *B* is the bandwidth of the channel and *S/N* is the signal-to-noise ratio. This result determines the probability of bit error for a given error correction code. The Shannon limit for FEC is defined as -1.6 dB [45]. Turbo codes are the only error correction codes that approach the Shannon limit for data transfer. In other words, turbo coding performance in a noisy channel (i.e. with multipath fading) approaches the performance of an AWGN channel (no multipath).

4.3.2 Forward Error Correction (FEC)

FEC coding is typically implemented before data modulation and spreading because it adds redundancy to the data stream. By adding redundancy to the data, errors in transmission do not have as much of an impact on correct demodulation as they do on uncoded data. Popular forms of FEC are convolutional coding and turbo coding. The performance of these codes is further enhanced by interleaving.

4.3.2.1 Linear Block Coding

Linear block codes are codes in which there are 2^n possible code words containing n bits, of which k are message bits and $(n - k)$ are redundant check – or parity – bits. A code word of length n bits containing k message bits is written in the format (n, k). The general form of a linear block code word, C, is

$$C = D \cdot G \tag{4.18}$$

where D is the k-bit message and G is a generator matrix. The generator matrix contains the results of a function that creates the parity check bits from the data bits. In linear block codes, there are 2^k valid messages, which lie within the larger set of 2^n code words. The code rate R, is the ratio k/n. For example, if a (7, 4) linear block code (rate 4/7) is used, there are 4 message bits and 3 parity bits. The code contains a total of 128 possible code words; however, only 16 codes contain valid messages. If an invalid codeword is received, the closest valid codeword is selected. Typical code rates for digital communication systems are 1/2 and 1/3.

4.3.2.2 Convolutional Coding

Convolutional codes are generated by a feedback shift register, similar to the m-sequence generator. This technique spreads the information content of the data among adjacent bits, allowing an error in any one output bit to be ignored without information being lost. The encoder's state transitions are known to the decoder, allowing the decoder to reconstruct the original bit stream. Errors are detected when the corresponding sequence of transitions could not have been sent. In the event an error is detected, the decoder constructs all possible tracks and selects the most appropriate. Convolutional codes provide better error correction performance than block codes. Figure 4.5 shows the E_b/N_o vs. BER for different coding schemes.

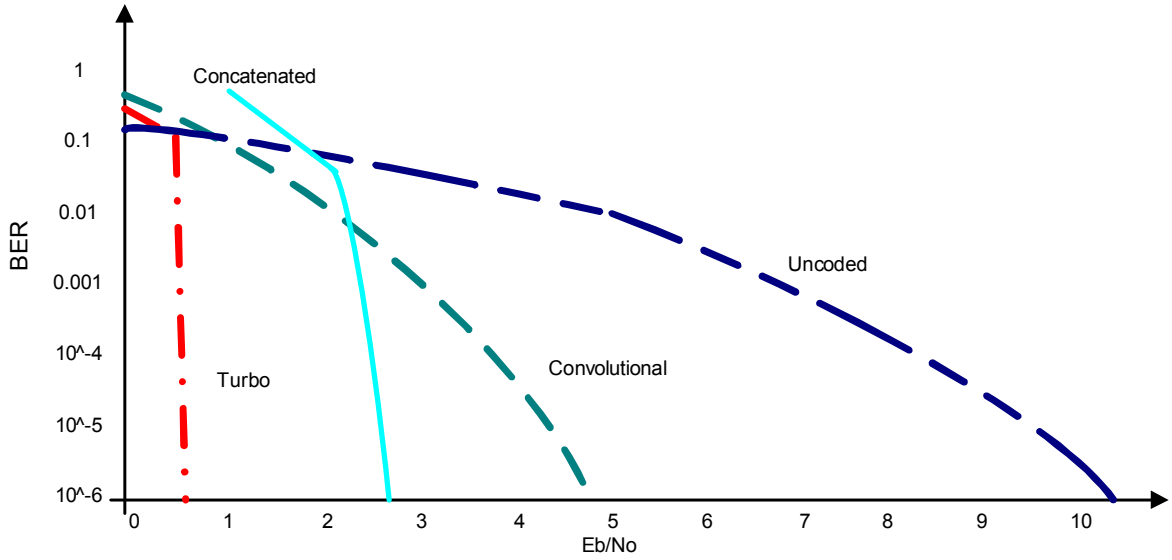

Figure 4.5 E_b/N_o vs. BER for different forward error correction codes: Turbo coding, Convolutional coding, Concatenated coding, and no coding. (From Figure 2 of [55], © The Aerospace Press. Reproduced with permission.)

4.3.2.3 Interleaving and Concatenated Coding

Concatenated coding refers to two error control coding operations implemented in series. Concatenated codes decrease the probability of undetected errors in the decoder. Typically, an interleaver is placed between the two stages of error control coding. An interleaver reads an encoded bit stream in by rows and outputs the bit stream in columns. A block diagram of concatenated coding with interleaving is shown below in Figure 4.6.

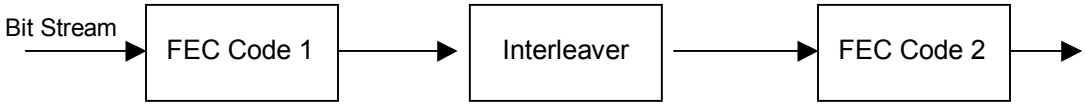

Figure 4.6: Concatenated Codes with Interleaver Block Diagram

Interleaving distributes data in such a manner to provide protection against burst errors, making it easier to recover data. At the receiver, the data is processed by a de-interleaver, which reconstructs the original message.

4.3.2.4 Turbo Coding

Originally introduced by [4], turbo codes are the most powerful codes currently available for error correction. A turbo code is the parallel concatenation of two or more convolutional codes, as shown in Figure 4.7. A typical application uses two encoders, interleaving the input to the second encoder with a block size on the order of hundreds of bits. Figure 4.3 depicts a rate-1/3 turbo encoder.

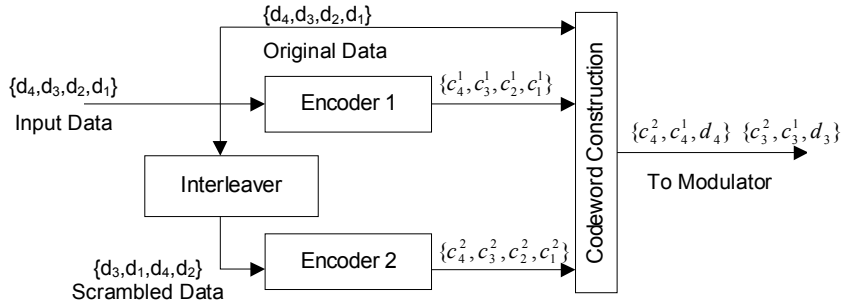

Figure 4.7. Turbo encoder block diagram. (From Figure 4 of [55], © The Aerospace Press. Reproduced with permission.)

While interleaving is typically used to spread contiguous bits among multiple blocks, interleaving has a different application in turbo codes. Interleavers in turbo codes interleave a data block within itself before outputting to the second encoder. The second encoder thus receives an interleaved version of the same data block the first encoder received, and generates an independent set of code bits. This application of interleaving provides a diverse coding sequence for transmission, which ultimately results in fewer errors.

At the receiver, the incoming bit stream is sampled to produce a soft decision – a continuous value that weights the confidence of each bit estimate. After the first decoder makes an initial soft decision, the second decoder receives that decision along with the incoming bitstream and produces a second soft decision. This process is repeated iteratively until the estimate approaches the maximum a-posteriori (MAP) estimate. The number of iterations performed is based on the data rate and the limits on system acquisition time. The original authors [4] show that 18 iterations are required to approach the MAP estimate; however, not all systems will require this much gain. Another method of decoding is the Viterbi algorithm, discussed in [22,30,59].

4.4 The Global Positioning System (GPS)

The Global Positioning System, or GPS, shares many of the same technical design challenges as the Globalstar System. The GPS system is presented to illustrate design strategies useful in the Globalstar System.

GPS was developed in the late 1970s by the Department of Defense to provide global navigation and timing. There are twenty-four satellites in six orbital planes in the constellation at an altitude of 20,200 km, putting the GPS satellites in medium earth orbit (MEO). The orbital period of a GPS satellite is 718 minutes, and the satellites are spaced such that at least four satellites are visible at any point on the surface of the Earth at any time. The mechanics of how GPS determines position is widely publicized, and is not discussed here. [45]

The GPS satellites use DS-SS to transmit position codes. There are two different codes – the C/A code (for course acquisition) and the Y code. The Y code is the encrypted P-code, a higher rate code that provides higher accuracy to authorized users. The C/A code is formed from the combination of two PN sequences of length 1023. This code has a clock rate of 1.023 MHz and repeats every millisecond. It is transmitted at 1575.42 MHz (the L1 frequency). The Y code has a clock rate of 10.23 MHz. The C/A and Y codes are used in quadraphase PN modulation of the L1 frequency, which results in a bandwidth of 2.046 MHz. The navigation message rate is 50 bps, and is modulated onto the C/A code such that one data bit covers 20 code sequences (20 ms) [38,45].

The orbital height and period of the GPS satellites gives a satellite velocity of 3.865 km/s. According to [45], when a GPS satellite is at the horizon, the angle between the velocity vector of the satellite and the position vector of a receiver is 76.1˚. Using equation 4.15 for the L1 frequency of 1575.42 MHz, this velocity and angle corresponds to a maximum Doppler shift of 4.872 kHz. However, this calculation ignores the effect of the earth's rotation on the Doppler frequency. The maximum Doppler spread (±4.872 kHz) can be reduced to ±4 kHz by assuming that the satellite must be at an elevation above 5˚ before the receiver can acquire a position.

Using 1 kHz steps, the receiver must search eight possible Doppler frequencies for each incoming signal.

In addition to detecting the correct Doppler shift, the receiver must also determine the correct start time (or time delay) for the locally generated PN sequence. Since the PN sequence is 1023 chips long and lasts 1 ms, the receiver must search over a 1 ms time spread in 1μs increments. These increments correspond to incrementing the local PN sequence one chip each correlation attempt [52].

The GPS system reduces the time required to search all possible signal locations (in time and frequency) by implementing an *Early-Late Gate Receiver*. This receiver has three timing paths: no chip delay, a half chip delay, and a half chip increment. A block diagram of a simplified early-late gate receiver is shown in Figure 4.8.

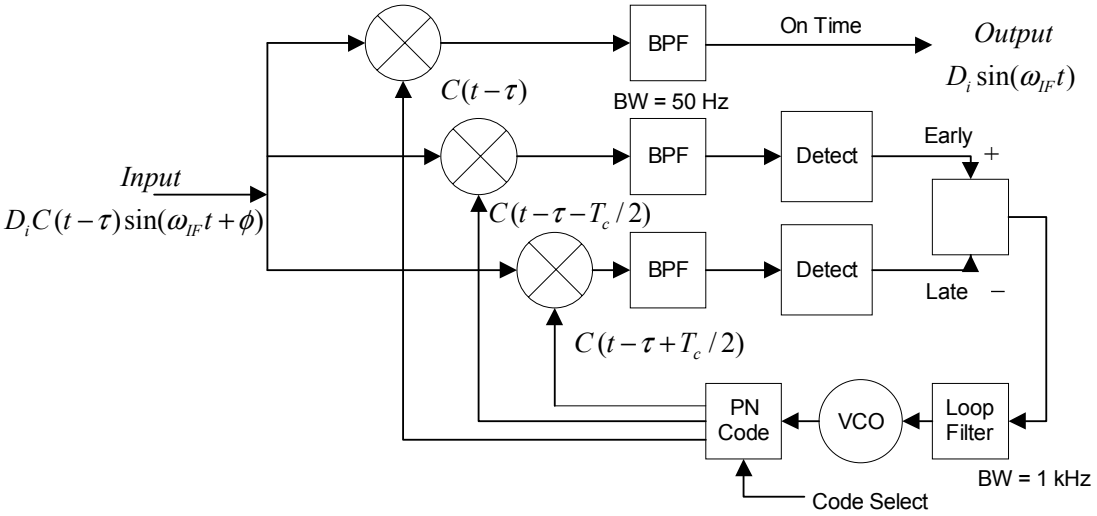

Figure 4.8. GPS Early-Late Gate Receiver Block Diagram

One major synchronization benefit of the GPS system is that the navigation message contains ephemeris data for the entire constellation. So once a receiver decodes the navigation message from one satellite, it can quickly locate all the other visible satellites using the data in the navigation message.

The Globalstar Satellite System does not have this advantage of transmitting ephemeris data with the message. Also, the early-late gate receiver would be difficult to implement for the

Globalstar system because of the extremely large search space dictated by the system parameters. Some aspects of the search space for the Globalstar system were discussed in Section 4.1.2. Methods for acquiring a signal from a Globalstar satellite are discussed in detail in Section 5.1.

Chapter 5

System Design and Simulation

The primary goal of this thesis is to design a beacon for transmitting data that minimizes physical size and required power (both transmit and supply). Simulating the receiver allows the design parameters of the transmitter to be fully defined. One important parameter derived from the simulation is the minimum transmit power necessary to complete the link. Knowing this, the transmitter can be designed to achieve that output power.

There are several important differences between the simulation presented here and the operation of an actual CDMA receiver. First, design challenges that applied to both the simulation and an actual receiver are presented. In Sections 5.1.2 and 5.1.3, the details and operation of a CDMA transmitter, and a receiver that could be implemented as a receiver for the Globalstar Satellite System are presented. Then in Section 5.2, the design and operation of the simulation and how it differs from the receiver of Section 5.1 are presented. For readers not familiar with MATLAB, the authors of [23] provide an excellent introduction to modeling communication systems in MATLAB.

The receiver was simulated in MATLAB; the goal of this simulation is to model the receiver on the Reverse Link of the Globalstar Satellite System to investigate the operation of the link. The Globalstar Satellite Communication link is described in detail in Chapter 3, Section 2. From this simulation, the lowest user transmit power required for the receiver to properly acquire the signal can be determined. In order to determine the lowest feasible user transmit power, the

system must first be modeled. Control cases are analyzed to validate the results of the simulation.

5.1. System Operation

The Globalstar Satellite System was described in detail in Chapter 3. In general, the system can be modeled by a transmitter, a channel, and a receiver, as shown in Figure 5.1. As discussed in Chapters 3 and 4, only the Reverse Link will be considered for this design.

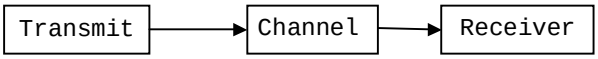

Figure 5.1. System Model: Globalstar Satellite System – Reverse Link, Transmit Only

The channel is usually modeled as Ricean fading for LEO satellite systems. According to [15,46,47] the Rician K-factors (or Rice factors), which quantify the ratio of the received signal power in a line-of-sight component to the received signal power in a multipath signal component, are in the range of 5 – 20 dB. However, the diversity gain from a Rake receiver allows the channel to be modeled as an Additive White Gaussian Noise (AWGN) channel. The reader interested in channel models should refer to [19,20,30] for more information. Because the Globalstar satellites have *bent-pipe* (or linear) transponders, the satellite can be considered part of the channel. As discussed in Section 3.2.2, the uplink C/N (transmitter to satellite) dominates the overall link C/N. Recall that this means that the overall C/N ratio at the receiver is limited by the uplink C/N ratio. For the simulation, the channel was modeled as an AWGN channel with the minimum C/N seen at the satellite.

Designing a receiver for the Globalstar Satellite System presents several challenges. The receiver must be able to handle both Doppler and time shifts. As derived in Section Chapter 3, the maximum Doppler shift is 31 kHz, and the variation in the time delay is 14 ms. The Doppler shift can be in either the positive or negative directions, significantly increasing the required search areas. The receiver must have a high sensitivity and a large coding gain, as the incoming signals will be well below the noise floor.

5.1.1. Design Challenges

Before the design itself is discussed, the challenges in realizing the design are presented. The two major challenges in the design of this system are the time delay and Doppler shift introduced by the motion of the satellite traveling above the earth. The effect of the position of the satellite relative to the Gateway receiver will be neglected because the time and frequency offsets can be calculated from the satellite ephemeris data. This calculation is possible for the receiver because it is in a fixed location, whereas the transmitter is mobile. The time delay is the amount of time it takes the transmitted signal to travel from the transmitter to the satellite to the receiver, and is a function of the position of the satellite relative to the transmitter. The Doppler shift, or frequency offset, of the signal is a function of the speed of the satellite relative to the transmitter. Both of these effects are discussed in greater detail below.

5.1.1.1 Doppler Shift

Doppler Shift is defined as the rate of change in signal phase over time relative to the receiver. In a LEO satellite system, Doppler shift can be introduced in the both uplink and downlink. In the uplink, the angle between the velocity vector of the satellite and the position vector of the transmitter directly impacts the level of Doppler shift seen at the receiver. In the downlink, the angle between the velocity vector of the satellite and the position vector of the receiver determines the amount of Doppler shift added to the signal. Equation 5.1 defines this relationship.

$$f_d = \frac{v}{\lambda}\cos\phi \qquad 5.1$$

In Equation 5.1, v is the velocity of the satellite, λ is the wavelength of the signal, and ϕ is the angle in degrees between the satellite velocity vector and transmitter (or receiver) position vector.

A receiver at the ground station would only need to consider the Doppler effect on the uplink because the receiver is stationary, so the Doppler effect on the downlink can be precisely calculated from the satellite ephemeris data and removed from the signal. The Doppler frequency shift on the uplink cannot be removed when the transmitted signal is being acquired

because the transmitter is mobile, and the location of the transmitter is typically unknown. If a prior position of the transmitter is known to the receiver, the correlator can estimate the Doppler shift from the last known position. This method can significantly reduce acquisition time if the transmitter has not moved too far between transmissions. Other methods of estimating the Doppler shift are presented in [19,20].

The unknown Doppler shift in the received signal presents an acquisition problem because the Doppler shift moves the signal away from the carrier frequency. The signal is arriving at the receiver with an unknown carrier frequency. Furthermore, the Doppler shift may change the timing of the symbols. The Doppler frequency is changing as the satellite moves across the sky. As presented in Chapter 3, the satellite velocity is 7.152 km/s; the uplink frequencies are 1610 – 1626.5 MHz and the downlink frequencies are 6875 – 7055 MHz. For the Globalstar system, the Doppler frequency offset in the uplink signal may transition from -31 kHz to +31 kHz in about 15 minutes. The transition is not linear; the frequency changes very little while the satellite remains near the horizon, but the frequency changes very quickly as the satellite approaches (and passes) zenith.

The range of frequency offsets is a function of satellite position relative to the transmitter, as defined in Equation 5.1. The maximum Doppler shift occurs when the satellite is on the horizon at the time of transmission, resulting in a ±31 kHz frequency offset. The minimum Doppler shift is 0 Hz, when the satellite is directly over the transmitter. This gives a frequency offset range of ±31 kHz. However, the Doppler shift can be either positive or negative in frequency, doubling the frequency range the receiver must search.

5.1.1.2 Time Delay

An acquisition challenge introduced by the varying distance of the satellite from the transmitter is signal time delay. It takes time for the transmitted signal to reach the satellite and then to be retransmitted back to the receiver. The path length the signal must travel between the transmitter and the satellite changes relative to the position of the satellite in the sky. The path length is greatest when the satellite is near the horizon, and the path length is least when the satellite is at zenith relative to the transmitter. These lengths can be calculated from basic geometry using the radius of the Earth and the orbital height of the satellite in view.

This varying time delay creates a problem for the receiver because the start time of the transmission is unknown. To reduce this variable, transmissions will be made at precise GPS times. The receiver will know to look for a signal within a time frame around the predetermined GPS transmission time. This time frame is defined by the variation in position of the satellite relative to the transmitter at the time of transmission. Since the transmitting frequency is relatively constant, the determining factor in time delay variation is the length of the path between the satellite and the transmitter. As described in Chapter 3, Section 2, the minimum total transmission delay is 9 ms, and the maximum total transmission delay is 23 ms, giving a delay range of 14 ms. This delay range corresponds to 17,192 chips of the transmitted CDMA code. Total transmission time is defined as the elapsed time between the transmission of the signal and the (expected) arrival of the signal at the receiver.

5.1.2. Transmitter

The transmitter has three primary sections: a GPS section, a control section, and an RF section. The GPS section has a GPS receiver for determining precise time and location. The location of the device is transmitted via the Globalstar satellite system, and the timing information is used to help synchronize transmissions. The control section of the transmitter determines the transmission start time and length and also contains the information required to interface with the Globalstar satellite system. The RF section of the transmitter formats the data from the controller and GPS receiver for transmission over the Globalstar channel. A block diagram of the receiver section of the transmitter is shown in Figure 5.2. The GPS and control sections are both microchips, so are not shown as block diagrams.

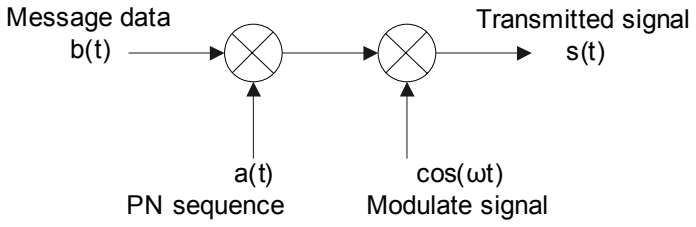

Figure 5.2. Block diagram of a generic RF section of a Globalstar transmitter. Both code and data modulation is BPSK, and the data is modulated with a carrier frequency of ω rad/sec. (Reproduced from [6] with permission.)

For a comparative analysis left to the reader, another approach to designing CDMA transmitter and receiver design is presented in [15]. The design parameters of the transmitter are defined as follows. A low data rate of 300 bps was selected to ensure the spreading gain would be large enough to overcome the system noise and interference. The existing Globalstar infrastructure supports convolutional forward error correction (1/2 rate with constraint length 7). Better performance may be obtained by implementing turbo coding for forward error correction; however, the receivers would need to be altered to accommodate this coding scheme. Coding is discussed in Section 4.3. As shown by the simulation results, a minimum transmit power of 0.25 W is feasible for correct system performance. Proper design of each section of the transmitter will minimize the supply power required to achieve this transmit power. Most RF transmitters are not very efficient, so a supply power of 2.5 W or 3 W could be required to achieve a transmit power of 0.25 W. An omni-directional transmit antenna with 0 dB gain is assumed in this design. Other design assumptions were presented in the link budget of Chapter 3, Section 2.2.

5.1.3. Receiver

The receiver for a Globalstar satellite transmission has several functions: acquisition, tracking, and demodulation. The receiver will operate off-line, analyzing the data after the entire transmission has been received. The receiver must first find the desired signal in the noise and then determine the frequency (Doppler) offset and time delay of the signal. After the receiver determines the correct Doppler offset and time delay, the desired signal is passed to a tracking loop. The tracking loop will maintain the correct frequency offset until the entire signal is demodulated. The tracking loop will prevent the receiver from losing the signal and needing to re-enter acquisition mode. A block diagram of the acquisition portion of the receiver is shown in Figure 5.3. The filter bank after the correlator determines the frequency of the carrier because the carrier frequency has been shifted by the Doppler frequency. If the despread signal has an SNR of 10 dB, then 48 filters with 1200 Hz bandwidths are needed to detect the signal.

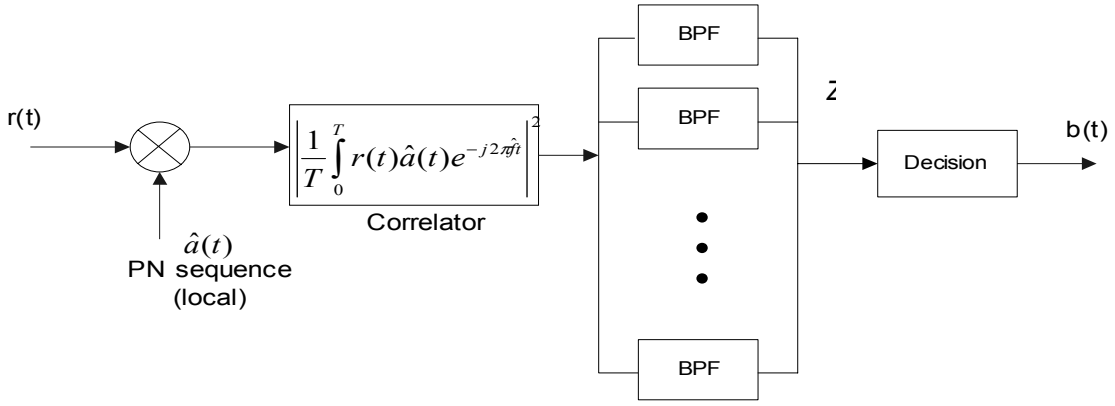

Figure 5.3. Block diagram of a Globalstar System receiver. The received signal is the transmitted signal plus noise from the channel: *r(t) = s(t) + n(t)*. The locally generated PN sequence, $\hat{a}(t)$, will not be correctly aligned with the transmitted PN sequence in either time or frequency. The decision device examines the output from the correlator (*Z*) and determines the correct code alignment. (Reproduced from [6] with permission.)

When beginning the acquisition process without a prior knowledge of the transmitter location, the receiver must first downconvert the signal to a suitable IF frequency before it can be decorrelated. The input signal, *r(t)*, in Figure 5.3 represents the received signal of Equation 4.14 down-converted to an IF frequency. Equation 4.14 defined the received signal as:

$$r(t) = \sqrt{2P}\,a(t-\tau)b(t-\tau)\cos(2\pi(f_c - f_d)t + \Theta) + n(t). \qquad 5.2$$

After the signal is downconverted, the received signal enters the code search loop. Search loops and strategies are discussed in Section 5.1.3.1. In Figure 5.3, $\hat{a}(t)$ represents the locally generated PN code sequence. The downconverted signal is multiplied by the first code, $\hat{a}_i(t)$. The correlator tests each time and frequency delay combination in the search space, and the decision device determines which – if any – of these delay combinations are correct. If none of the delays tested result in a positive match, the receiver multiplies the demodulated IF signal by the second code, $\hat{a}_{i+1}(t)$, and repeats the search process. The search is repeated for all possible codes, $\hat{a}_n(t)$, until a positive match is found. When the time delay is determined, the spreading code, *a(t)*, and the time delay, τ, will be canceled from Equation 5.2. The filter bank of Figure 5.3 will determine the Doppler frequency, f_d, which will allow the message, *b(t)*, to be demodulated. This process of searching through time, frequency, and code space is referred to as acquisition, and is described in the following section.

5.1.3.1 Acquisition

The first function the receiver must perform is acquiring the signal. The simulation presented in Section 5.2 and Chapter 6 will determine the minimum required user transmit power; the link budget of Section 3.2.2 showed that the uplink C/N is the limiting factor in acquiring the transmitted signal. In order to properly acquire the signal, the receiver must search through all possible time delays and frequency offsets. As mentioned in Section 5.1.1, the range of possible Doppler shifts is 64 kHz, and the range of possible time delays is 14 ms. The largest step sizes are 300 Hz (in frequency) and 0.8 μs (in time). Using these increments and ranges, the receiver would need to search close to 4 million possible combinations of time and frequency delay to retrieve the signal from the noise.

The search space can be reduced in several ways. It is unfeasible for the minimum time delay and the maximum frequency offset to occur at the same time. This is because the minimum time delay occurs when the satellite is at zenith. When the satellite is at zenith, there is no Doppler shift. Likewise, it is not possible for the minimum frequency offset to occur at the same time as the maximum time delay. The maximum time delay occurs when the satellite is on (or near) the horizon; the corresponding Doppler shift for a small elevation angle is approximately 30 kHz. There are several other combinations that have extremely low probability of occurring. For example, when the satellite is close to zenith (within 5°), the frequency offset will be relatively small compared to the maximum frequency offset, and the time delay will be relatively short compared to the maximum time delay. This reasoning is more difficult to apply when the satellite is near the horizon because the Doppler shift changes very quickly, but the time delay does not change at the same rate.

Using this knowledge, the search space can be reduced by at least 30 %. In [54] search strategies and probability distributions are presented for LEO satellite Doppler offsets. Using the parabolic probability density function (PDF) of [54], the most likely Doppler offsets can be found, and the receiver can begin searching in the most likely areas to reduce acquisition time.

There are two core classes of algorithms for searching the possible values of time and frequency offsets – serial and parallel. Both classes attempt to locate the signal by running the correlator at each frequency offset at predetermined increments of time. In a serial search, the delays (in both time and frequency) are run sequentially, and the set of delays that produces the

maximum output from the correlator is taken to be the correct time and frequency. In a parallel search, the delays (in both time and frequency) are all run at the same time. This type of parallel search requires one correlator for each possible delay, while a serial search requires only one correlator. The difference between these strategies is the trade-off between acquisition time and complexity. The strategy utilized in the simulation is discussed in Section 5.2.

5.1.3.2. Tracking

The tracking loop in a spread-spectrum receiver has two purposes: to maintain lock on the signal and to bring the code into a closer alignment. In general, the acquisition loop will align the code within a chip or half a chip. The tracking loop will align the code within an eighth or a sixteenth of a chip. Splitting the alignment process this way minimizes acquisition time while allowing for the most precise performance possible. The reason that the code needs to be aligned to within an eighth of a chip (or better) is that the actual range of time and frequency delays is continuous; however, these ranges are discretized to create a finite search space. A tracking loop is not implemented in the simulation.

5.2. Simulation Design

The goal of this simulation is to determine the minimum transmit power required for the receiver to correctly locate the transmitted signal. The simulation was performed in MATLAB. Because of memory limitations in MATLAB, two simulations were created to model different aspects of the Globalstar receiver. First, the performance of the receiver in noise was simulated to establish system benchmarks. The results of this simulation are presented in Section 6.1. Then, the performance of the correlator in the presence of noise as well as time delays was simulated. A brief exercise was performed to verify that the correlator could not locate the signal if the modulation frequency is incorrect. The results of the correlator performance simulation are presented in Section 6.2.

5.2.1 Simulation Models

As discussed in Chapters 3 and 4, the Globalstar Satellite System uses a m-sequence of length 131,072 [40] on the reverse link. The Globalstar sequence length gives a spreading gain of 36 dB for the 300 bps data rate assumed in this design. Equation 5.3 shows the relationship between the spreading gain, N, and the bit duration, T_b.

$$N = \frac{T_b}{T_c} \tag{5.3}$$

In Equation 5.3, the bit duration, T_b, is the inverse of the data rate (300 Hz). The chip duration, T_c, is the inverse of the chip rate (1.228 Mcps). Using these values, the spreading gain (N) is 4093, or 36 dB. The spreading gain of both simulations is less than that of the Globalstar Satellite System, as shown below.

The performance of this code in noise was modeled by using a signal formed from a long string (12,700 chips) of randomly distributed binary numbers in the set [-1, +1]. An integration time of 127 chips was used for this performance simulation, which gives a spreading gain of 20 dB. The results of the noise performance simulation are presented in Section 6.1 and represent the control cases used to verify the results of the correlator performance simulation.

To model the performance of the Reverse link under time and frequency delays, an m-sequence of length 2046 was used. The correlator integrated over the entire code (integration time of 2046 chips). This resulted in a spreading gain of 33 dB, which is only 3 dB below the spreading gain of the Globalstar System.

All simulations were run for two separate cases: the best case and the worst case. The best case simulated was only one user accessing the satellite transponder. This case was analyzed for C/N ratios of –3.7 dB and –8.5 dB. Much more time was devoted to analyzing the worst-case scenario discussed below.

Table 5.1 shows the C/N ratios calculated in Section 3.2.2 and the corresponding transmit powers for a single user. The C/N ratios of Table 5.1 represent the overall C/N ratio seen by the receiver in clear air conditions for a single user accessing the satellite transponder.

Transmit Power	C/N
2 W	0.5 dB
1 W	-2.5 dB
0.75 W	-3.7 dB
0.5 W	-5.5 dB
0.25 W	-8.5 dB

Table 5.1. Transmit Power and corresponding single user overall C/N at the receiver.

The simulations for the worst-case scenarios considered the effect of interference from many users accessing the satellite transponder at the same time. This type of interference is referred to as multiple access interference, or MAI. When many signals are present in the satellite transponder at the same time, they interfere with each other. There are several methods of reducing multiple access interference, referred to as *interference suppression*; several of these methods are discussed in [15].

As discussed in Section 3.2.2.2, mutual interference in a CDMA system can be treated as AWGN. With this treatment, the interference (I) is added to the thermal noise (N) in the C/N ratio resulting in a new ratio: the C/(N+I) ratio. For the beacon transmit powers tested in the simulation, the magnitude of the interference was much larger than the magnitude of the thermal noise. Therefore, the interference power level dominates the C/(N+I) ratio; the C/(N+I) ratio is referred to as the C/I ratio.

In the multiple user case, the number of users described below is *per* spot beam (or footprint). Each satellite has 16 spot beams, and there are 48 satellites in the constellation. The maximum number of users referred to in this analysis is per spot beam and not for the entire Globalstar Satellite System. Three multiple user cases were simulated:

1. Maximum Load: 165 users (100% capacity),
2. Heavy Load: 140 users (85% capacity),
3. Average Load: 83 users (50% capacity).

The *users* in the multiple user cases are Globalstar cellular customers. The average EIRP for a cellular transmission is –9.4 dBW, and the maximum cellular transmit EIRP is –4 dBW [11]. The average transmit EIRP was used in interference calculations. For the simulations, the transmit power of the beacon was varied between 50 mW and 0.25 W for each multiple user case

listed above. The C/I ratio was calculated for beacon transmit powers between 0.5 W and 2 W for the 100% capacity case. The results for these transmit powers in the multi-user case were interpolated from both the single-user case results and the lower transmit power results of the multiple user analysis. Table 5.2 summarizes all of the C/I values calculated for a multiple user environment.

Number of Cellular Users	Beacon Transmit Power	C/I
165	2 W	-9.7 dB
165	1 W	-12.8 dB
165	0.75 W	-14 dB
165	0.5 W	-16 dB
165	0.25 W	-18.8 dB
165	0.1 W	-22.7 dB
165	75 mW	-24 dB
165	50 mW	-25.8 dB
140	0.5 W	-15 dB
140	0.25 W	-18 dB
140	0.1 W	-22 dB
140	75 mW	-23.3 dB
140	50 mW	-25 dB
83	0.5 W	-12.7 dB
83	0.25 W	-15.8 dB
83	0.1 W	-19.7 dB
83	75 mW	-21 dB
83	50 mW	-22.7 dB

Table 5.2. Carrier-to-Interference ratios for varying beacon transmit powers under different system loads. The system loads are: maximum capacity (165 users), heavy load (140 users), and average load (83 users).

All simulations were performed under the following assumptions:

1. If the receiver can properly acquire the transmitted code, the data can be properly received.
2. Because the statistical properties of Gold codes approximate those of random sequences, the spreading code can be represented by a sufficiently long string of random binary numbers in the set [-1, +1].
3. A sample set of data can be used to approximate results for the set.
4. All users are uniformly distributed in the satellite beam.
5. The satellite beam is roughly circular and flat (two dimensional) over the area of interest.
6. The effect of the Earth's rotation on the Doppler frequency is neglected.

These simulations employed a parallel search. Each feasible time delay (as discussed above) was tested for each frequency delay in the search space. The time increment for this simulation was 1 chip (0.8 μs), and the frequency step was 300 Hz. No threshold was used for this simulation; the results of each correlation were stored, and the position of the maximum output from the correlator was selected as indicating the correct code alignment.

5.2.2 Simulated Receiver Model

As described in Section 5.1, the receiver simulated for this thesis has several important differences from the receiver in Figure 5.3. The dotted line in Figure 5.4 shows the portion of the receiver that was implemented in this simulation.

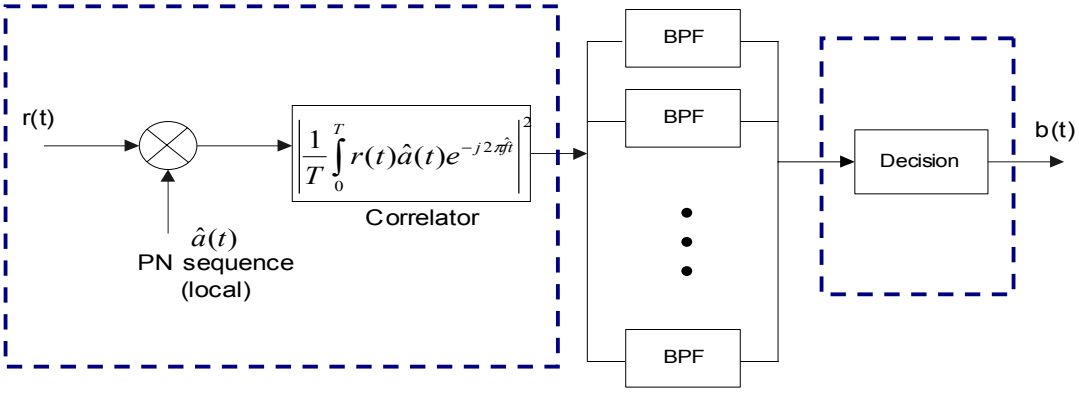

Figure 5.4. Block diagram of simulated Globalstar system receiver. The portions of the receiver inside the dashed lines were the only portions of the receiver simulated. Because of this, the decision statistic relies only on the output of the correlator, rather than the combined outputs of both the correlator and the filter bank. The decision device examines the output from the correlator (Z) and determines the correct code alignment.

The first major difference between the receivers of Figures 5.3 and 5.4 is that the Globalstar receiver of Figure 5.3 operates at an IF frequency. The simulated receiver of Figure 5.4 operates at baseband. For this reason, the effects of Doppler shift of the carrier frequency could not be properly observed. Also, the additional effect of the Doppler shift on the chip timing of the spreading sequence could not be properly observed. The relationship between the Doppler shift and the code rate is shown in Equation 5.3:

$$f_{clock} = \frac{R_c}{f_c} f_d \tag{5.3}$$

where f_d is the Doppler shift, f_c is the carrier frequency, R_c is the chip rate, and f_{clock} is the resulting shift of the clock frequency. For the Globalstar System parameters presented thus far – a chip rate of 1.228 Mcps, a maximum Doppler shift of 31 kHz, and an uplink carrier frequency of 1610 MHz – the maximum clock frequency shift is 24.6 Hz. For the Globalstar PN code length of 131,072, this translates to a shift of one chip every 235 chips. These two effects from Doppler shift are areas for further study.

Unlike the Globalstar system, the simulation did not utilize any coding or interleaving. Because the timing delays were tested in one chip increments, the simulation assumed that the timing delay of the received signal would be an integer number of chips. In the Globalstar receiver, the correlator should use ½ chip (or smaller) increments for better performance. Using ½ chip increments effectively doubles the search space, but is a worthwhile trade for better receiver performance.

Another consideration not taken into account in the simulation is the effect of frequency offset on integration time, since frequency offsets were not implemented in the simulation. For good correlator performance, the inverse of the integration time ($1/NT_c$) should be much larger than the frequency offset. If this relationship is not preserved, the frequency offset will change the phase of the signal during correlation, resulting in serious degradation to correlation performance. This simulation also assumed coherent integration; that is, the correlation integral is calculated over the entire integration period. In cases of frequency offset, non-coherent integration may need to be implemented in the correlator to maintain the proper relationship between integration time and frequency offset. In non-coherent integration, several shorter integrations are performed and summed to total the required integration time. For example, this simulation integrates over the entire code length, which is an integration time of 2046 chips. If a frequency offset dictated that this integration time was too long, six (coherent) integrations over 341 chips could be summed to achieve a total (non-coherent) integration time of 2046 chips. Using non-coherent integration to reduce coherent integration time results in a slight performance degradation, but its benefits over frequency offset outweigh this degradation.

5.2.3 Simulation Implementation

The simulations produced significant results that were aligned with the results expected from theory. The two simulations were introduced in Section 5.2.1; the methodology behind the simulations is explained in detail here.

The first simulation for examining receiver performance for a single transmitter utilized a random code that is long (12700 chips) relative to the integration time (127 chips). After the code was generated, noise was added to the signal. The level of noise added corresponded to the single user C/N ratios in Table 5.1: 0.5, -2.5, -3.7, -5.5, and -8.5 dB. Because the noise level was increased rather than reducing the signal level, the value of the decision statistic at the output of the correlator increased in proportion to the noise increase. For each signal level, the correlator performed the following steps.

First, the correlator performed the integration shown in Equation 5.4 for the first 127 chips in the sequence.

$$Z = \left| \int_0^{127} r(t)\,\hat{a}(t)\,dt \right|^2 \qquad 5.4$$

The result of the integration – the decision statistic, Z – was stored, the position of the code sequence was incremented by 127 chips (one integration interval), and the correlator performed an integration on the next section of 127 chips. This process was repeated until integrations of length 127 were completed for the entire data stream (12,700 chips). The correlator then searched the stored statistics for the maximum value and chose that value as the correct code position. The output from the correlator, Z, is referred to as the decision statistic, because it is used to determine the time delay of the incoming code. This simulation was run 1000 times for each C/N ratio. The results of these simulations are discussed in Section 6.1.

The second simulation examined correlator performance when the desired signal was transmitted with other users' signals, and the desired signal was delayed in time. The multiple-user cases are described above in Section 5.2.1. Three time delays were arbitrarily chosen: 20 chips (16 μs), 100 chips (80 μs), and 399 chips (0.318 ms). For these simulations, the integration time (NT_c) was equivalent to the code length (2047 chips or 1.64 ms). The simulator was run at worst case carrier-to-interference ratios (-20 dB, -22 dB, -24 dB, and -26 dB) for these arbitrary

time delays. The beacon transmit power levels corresponding to these C/I ratios for the various multiple-user cases simulated are summarized in Table 5.2. The C/I ratios above –20 dB in Table 5.2 were not simulated because they are assumed to perform adequately. This assumption is explained further in Section 6.1.

For the simulations presented in Chapter 6, the correlator performed the following operations, independent of the received signal power level. First, an m-sequence of length 2046 was generated. Then the arbitrary time delay was added before the beginning of the sequence, and noise was added to the resulting data stream. As in the first simulation, the noise level was increased rather than decreasing the signal level. Because of this approach, the decision statistic at the output of the correlator increased relative to the increase in noise.

To simplify the simulation, the correlator only had to search 512 possible time delays. The correlation performed the integration of Equation 5.5 and stored the results.

$$Z = \left| \int_0^{512} r(t)\hat{a}(t)dt \right|^2 \qquad 5.5$$

After the correlator had tested all 512 possible time delays, it searched the stored decision statistic (Z) values and chose the position with the maximum value as the correctly aligned time delay. Initially, the number of simulations was set to 1000; however, the first several groups of simulations demonstrated that 500 simulations produced the same statistical results as 1000 simulations. The results of these simulations are discussed in Section 6.2.

5.3 Conclusions

This chapter presented the design and implementation of the simulation utilized in this thesis to determine the minimum required transmit power for satisfactory receiver performance. The first section of this chapter presented the design challenges for acquiring the transmitted signal, including Doppler frequency shifts and time delays. The theory behind the operation of

the receiver was discussed as well as the two primary functions of the receiver: acquisition and tracking.

In the second section, differences between the simulated receiver and an actual Globalstar system receiver were highlighted; the simulation only implements a portion of the system receiver. The two cases simulated were discussed in Section 5.2.1: the best-case (or ideal) scenario of only one beacon accessing the satellite with no cellular users and the worst-case scenario of a beacon accessing the satellite at the same time as the maximum number of cellular users (165) in a single spotbeam. The results of the simulation and a discussion of the results are presented in Chapter 6.

Chapter 6

Simulation Results

Chapter 5 introduced the design and operation of the transmitter and receiver as well as the design and methodology of the receiver simulations. This chapter examines the results of those simulations described in Chapter 5 to determine the performance of the correlator in the presence of noise and when the received signal is delayed in time. For the simulation, the search space was restricted to 512 possible time delays (in chips), with a 1 chip increment size. Chapter 5 discusses the larger search space required to implement a Globalstar system receiver, as well as other design considerations.

Performance will be analyzed based on the ability of the correlator to correctly determine the time delay (or start position) of the transmitted code. The correlator runs a parallel search strategy with no threshold, so the maximum value after all positions have been tested is taken as the position of the signal. An error is defined as the incorrect determination of time delay or frequency offset by the correlator. Error rate is defined as the number of incorrect time delay selections made by the correlator divided by the total number of simulations.

Section 6.1 presents the results of the simulation of the correlator in the presence of additive white Gaussian noise (AWGN) for a single user accessing the satellite transponder. Section 6.2 presents the worst-case results of the simulation of the correlator in the presence of a time-shifted received signal with multiple user access interference (MAI), and Section 6.3 presents a probability of detection analysis and an estimate of the mean acquisition time.

6.1 Single User Simulation Results

As discussed in Section 5.1, the first simulation examined the performance of the correlator in the presence of increasing levels of AWGN for a single transmission. First, the correlator performance was examined for a single beacon transmitting at varying power levels of 2 W, 1 W, 0.75 W, 0.5 W, and 0.25 W. Although it is not likely that only one transmitter will be in the satellite transponder during an arbitrary time period, these results are useful both as reference cases and for determining multiple access interference levels.

Transmit Power	Single User C/N
2 W	0.5 dB
1 W	-2.5 dB
0.75 W	-3.7 dB
0.5 W	-5.5 dB
0.25 W	-8.5 dB

Table 6.1. Transmitter power levels and corresponding C/N values for a single user occupying the satellite transponder.

According to [8], the Globalstar Satellite System can support up to 165 simultaneous cellular phone links within a single cell, where a cell refers to the portion of the satellite footprint from a single spot beam. This calculation is based on the energy per bit required for a 0.01 probability of bit error for voice communications. According to [11], Globalstar cellular phones have an average transmit EIRP of –9.2 dBW. Additional information on capacity calculations for CDMA systems is available in [15, 18].

Because the transmission start times and interval from each beacon are tied to a GPS clock, the transmission times of each beacon can be controlled so that only one beacon is transmitting within a single footprint at any time. (The transmission timing can be controlled for a limited number of beacons; however, the number of beacons deployed within a single footprint is expected to be very small.) Therefore, the probability that two of beacons transmit at the same time is zero, because the transmit times are controlled to avoid overlaps. Even though the beacon transmissions can be regulated, the Globalstar system cellular user transmissions are not regulated and must be taken into account. It is reasonable to assume that the Globalstar system will not allow any devices to access the satellite once capacity (165 users) has been reached.

However, it is unlikely that the Globalstar system is at 100% capacity a majority of the time. For this thesis, heavy satellite loading is defined as 85% of system capacity (140 concurrent transmissions), and average loading is defined as 50% of system capacity (83 concurrent transmissions).

For an average cellular transmit EIRP of –9.4 dBW [11] and a thermal noise power of 169.6 dB, the C/(N+I) ratios were calculated for each of the system loading levels defined above: maximum loading (100% of system capacity), heavy loading (85% of system capacity), and average loading (50% of system capacity). As discussed in Equation 3.6 of Section 3.2.2.2, the C/(N+I) ratio is calculated as:

$$\frac{C}{N+I} = 10\log\left(\frac{C}{N_t + C(Q-1)}\right) \qquad 6.1\ [45]$$

where C is the transmit power of the desired signal (in this case, the beacon transmit power), Q is the number of users accessing the satellite, and N_t is the thermal noise of the link. Table 6.2 presents the results of Equation 6.1 for the three levels of system loading (maximum, heavy, and average) at different beacon transmit powers, ranging from 50 mW to 2 W. The higher beacon transmit power levels are considered for heavy loading, and the lower beacon transmit power levels are considered for average loading.

Number of Cellular Users	Beacon Transmit Power	C/(N+I)
165	2 W	-9.7 dB
165	1 W	-12.8 dB
165	0.75 W	-14 dB
165	0.5 W	-16 dB
165	0.25 W	-18.8 dB
165	0.1 W	-22.7 dB
165	75 mW	-24 dB
165	50 mW	-25.8 dB
140	0.5 W	-15 dB
140	0.25 W	-18 dB
140	0.1 W	-22 dB
140	75 mW	-23.3 dB
140	50 mW	-25 dB
83	0.5 W	-12.7 dB
83	0.25 W	-15.8 dB
83	0.1 W	-19.7 dB
83	75 mW	-21 dB
83	50 mW	-22.7 dB

Table 6.2. Resulting C/(N+I) ratios for varying beacon transmit power at three levels of system loading: maximum capacity (165 users), heavy loading (140 users), and average loading (83 users). The cellular users transmit at an average EIRP of –9.4 dB, which is regulated by the Globalstar gateways.

Both the single user results and the results of the multiple user access case are presented in the remainder of the chapter. The performance of the correlator was significantly reduced in the presence of high levels of interference as the transmitted signal became overwhelmed by the multiple access interference. This section presents results for C/N and C/I ratios above –20 dB in Tables 6.1 and 6.2 for both the single user and multiple user cases. Section 6.2 presents the *worst-case* results for C/I ratios below –20 dB in Table 6.2. The multiple user cases with C/I ratios above –20 dB are assumed to provide acceptable system performance based on interpolating between the worst-case results and the single user results.

It follows intuitively that the error rates for the single-user C/N values in Table 6.1 (0.5, -2.5, -3.7, -5.5, and -8.5 dB) are all 0 % since the error rate for a C/N of –8.5 dB is 0 %. As shown below, the error rate for a C/I ratio of –20 dB is 20% on average. This is an acceptable for some applications; therefore, it is assumed that C/I ratios above –20 dB will provide acceptable performance for some applications. The worst-case multiple user access case provides more insight into the operation of the system than other cases. The majority of transmissions will not be subjected to worst-case conditions, so acceptable system performance at worst-case C/I ratios guarantees satisfactory system performance at higher C/I or C/N ratios.

As discussed in Section 3.2.2.2, the interference increases with the number of simultaneous users in the system. This interference adds to the noise level and lowers the carrier-to-noise-plus-interference ratio (Equation 3.6). In the cases described in Table 6.2, the interference power level was much greater than the thermal noise power, so the resulting C/(N+I) values can be treated as C/I values.

6.2 Multiple User Simulation Results

This section presents the simulation performed to observe the performance of the correlator when the received signal was shifted in time. Three arbitrary time delays were simulated: 20 μs (25 chips), 80 μs (100 chips) and 0.318 ms (398 chips). The simulation results presented in Section 6.1 were used to verify the results of this simulation.

As described in Section 5.2, this simulation transmits an m-sequence of length 2046 over an AWGN channel. (One chip is 0.8 μs wide, corresponding to a chip rate of 1.228 MHz.) Before noise is added to the signal, an arbitrary time delay is added to the beginning of the data stream. The correlator must determine the correct time delay in order to remove the spreading code. An integration time equal to the code length was used (2046 chips). The search space was restricted to time only, with a total of 512 possible chip delay positions and an increment size of 1 chip. Therefore, the arbitrary time delays were also restricted to a maximum of 512 chips.

The simulation was performed in MATLAB, and MATLAB has no zero position delay. Therefore, for a 100 chip delay, the maximum correlator output should correspond to a delay of 101 chips. Similarly, a 398 chip delay will correspond to a maximum correlator output at a 399 chips delay in the MATLAB correlator.

The results of each arbitrary time delay are presented and discussed in the following order: 20 chip delay, 100 chip delay, and 399 chip delay. These results demonstrate the ability of the correlator to determine the correct code alignment for an arbitrary time delay. Although not realistic in the sense that the received signal will not have a time delay without a corresponding

frequency shift, this simulation was performed to observe the performance of the correlator under time delay conditions independently from Doppler frequency offset conditions.

6.2.1 A time delay of 20 chips (16 μs)

The first simulation executed to observe the performance of the correlator when a time delay is added to the message implemented an arbitrary time delay of 16 μs, which corresponds to 20 chips at the 1.228 Mcps chip rate. Recall that an m-sequence of length 2046 is used as the transmitted data, and the integration time is 2046 chips. The effects of Doppler shift are not examined in this set of simulations.

This simulation focused on the multiple user access case for a fixed user transmit power of 0.75 W (-1.3 dB). The C/I values of -20, -22, -24, and –26 were tested during this simulation. Table 6.3 shows the system loading levels and beacon transmit powers that correspond to each C/I value simulated.

		Number of Cellular Users		
		165 users	140 users	83 users
C/I ratios	-20dB	0.25 W	0.25 W	0.1 W
	-22 dB	0.1 W	0.1 W	75 mW
	-24 dB	75 mW	75 mW	50 mW
	-26 dB	50 mW	50 mW	25 mW

Table 6.3. Beacon transmit power levels for simulated C/I ratios at different levels of system loading: maximum capacity (165 users), heavy loading (140 users), and average loading (83 users).

For an overall carrier-to-interference ratio of -20 dB at the receiver, 100 simulations produced 22 errors. An error is defined as a simulation in which the correlator chooses a time delay other than the true (or transmitted) time delay. The *error rate* is defined as the percentage of *errors* in each set of simulations with the same parameters. Using this definition of error rate, the detection rate is equal to one minus the error rate.

From these definitions, the error rate for the 20 chip delay case is 22%. The performance level may be acceptable in some cases. For instance, if an application only requires information if the tracked object is moved, it would not be necessary to receive every transmission and 80% of transmitted locations may provide sufficient data to determine if the tracked object was moved. However, for applications requiring more frequent location updates,

a –20 dB C/I ratio may not be sufficient. Some changes that could be made in the correlator to improve performance are discussed in Section 6.2.4. The error rates for all of the C/I ratios simulated are summarized in Table 6.4. Refer to Table 6.3 for the beacon transmit power levels and number of cellular users that correspond to the received C/I values in Table 6.4.

Received C/I	Detection Rate	Error Rate
-20 dB	78%	22%
-22 dB	47%	53%
-24 dB	30%	70%
-26 dB	14%	86%

Table 6.4. Results of simulation to observe correlation performance for multiple users with an arbitrary data delay. *Detection Rate* is the percentage of correct time delays chosen by the correlator. *Error Rate* is the number of errors divided by the total number of simulations. The simulation parameters were an arbitrary time delay of 16 μs (20 chips), a transmitted m-sequence of length 2046 chips, and an integration time of 2046 chips.

To achieve a detection rate of approximately 80%, a received C/I of –20 dB is required. The beacon transmit power levels that would achieve this detection rate are 0.25 W under maximum system loading (165 users), 0.25 W under heavy system loading (140 users), and 0.1 W under average system loading (83 users). For the C/I ratios simulated in this case, the error rates are acceptable for the transmitted beacon power levels. To transmit at power levels below 0.25 W, other correlation methods, such as non-coherent integration or a Rake receiver, should be implemented. According to theory, these methods should achieve better performance for low transmit power levels at the C/I ratios in Table 6.4.

6.2.2. A time delay of 100 chips (80 μs)

The next set of simulations performed introduced an 80 μs (100 chip) delay to the transmitted m-sequence. Recall that the purpose of this group of simulations is to observe the performance of the correlator when an arbitrary time delay is introduced to the transmitted data. The same simulation parameters of an m-sequence length of 2046 and an integration time of 2046 chips are maintained. The effects of Doppler shift are not examined in this set of simulations. Recall that rather than comparing the correlator output to a threshold, the maximum output from the correlator was chosen as the correct time alignment.

In addition to the C/(N+I) ratios (-20, -22, -24, and -26 dB), two of the single user C/N ratios were also simulated. The single user C/N ratios simulated were –3.7 dB and -8.5 dB, which correspond to transmitter power levels of 0.75 and 0.25 W, respectively. The results of the single user C/N ratios are presented first, and then the results of the multiple user C/(N+I) ratios are summarized. As discussed in Section 6.1, the C/(N+I) ratios are actually closer to C/I ratios because the magnitude of the interference is much larger than the magnitude of the thermal noise for the C/(N+I) ratios listed above.

Figure 6.1 shows the results for a typical simulation with an 80 μs (100 chip) time offset, a C/N of -3.7 dB, and no Doppler shift. The C/N corresponds to a transmit power of 0.75 W for a single user accessing the satellite. The correlator output in Figure 6.1 is normalized with respect to the maximum correlator output.

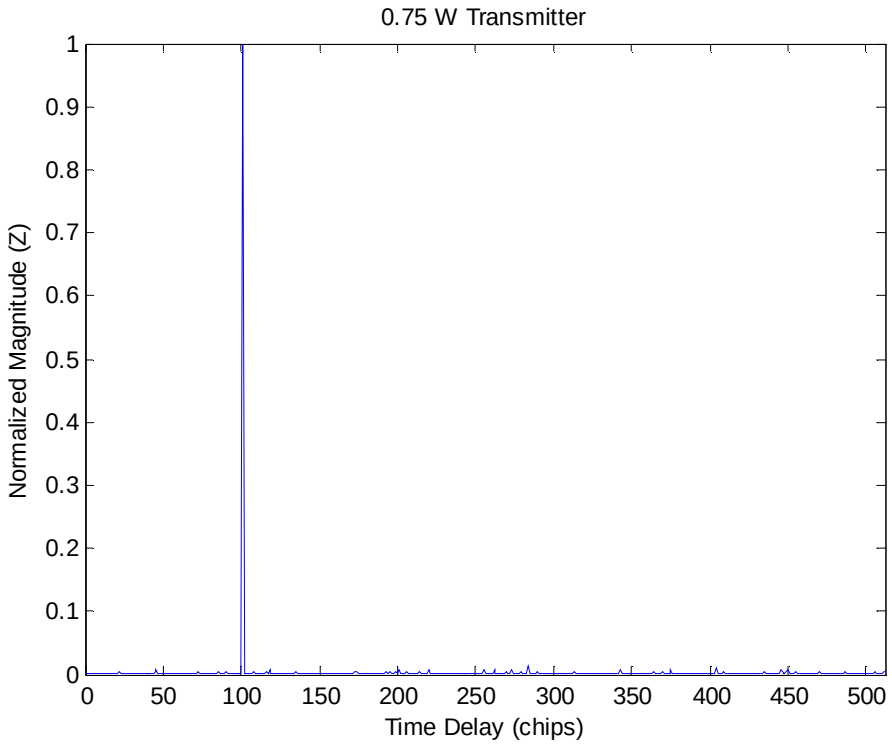

Figure 6.1. Output of correlator for a single user with known code with 100 chip time shift and no Doppler shift. The code length was 2046, the integration time was 512 chips, and the C/N was -3.7 dB. The correlation peak is at NT_c=101 chips, as expected.

The sample simulation result shown in Figure 6.1 approximates the ideal cross-correlation properties defined in Section 1 of Chapter 4. This result implies that correlator

performance for a single user at C/N ratios of -3.7 dB or higher will be excellent. Next, a single user C/N ratio of -8.5 dB, which corresponds to a transmit power of 0.25 W, was simulated with the same parameters. Figure 6.2 shows a typical output of the correlator for one simulation. The magnitude of Figure 6.2 is normalized with respect to the maximum correlator output.

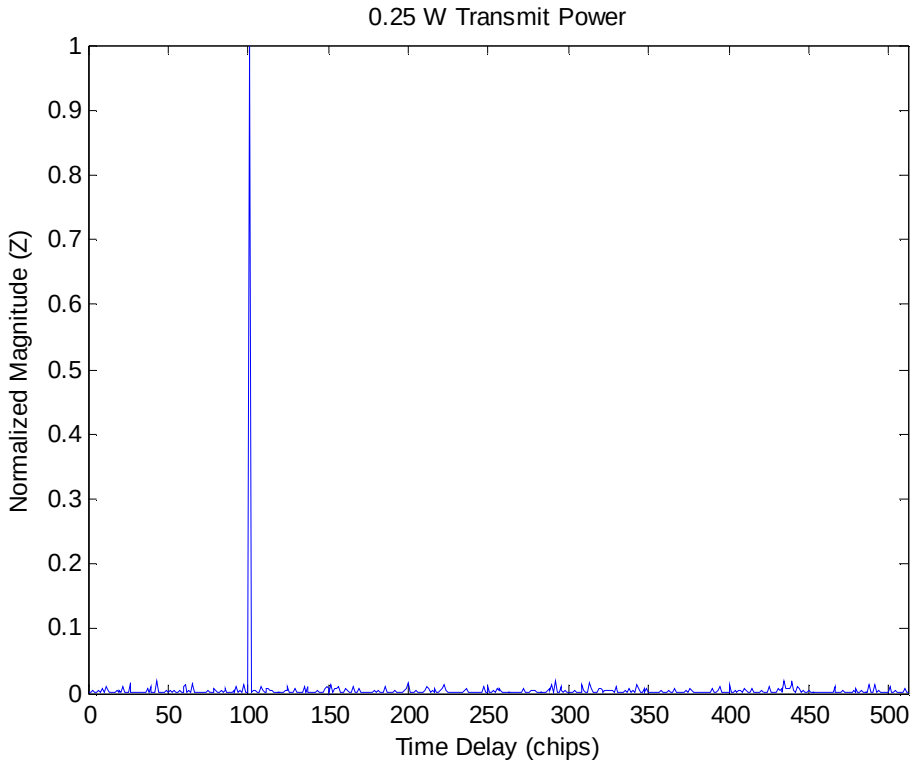

Figure 6.2. Output of correlator for a single user with a known code with a 100 chip time shift and no Doppler shift. The code length was 2046, the integration time was 512 chips, and the C/N was -8.5 dB, which corresponds to a 0.25 W transmit power. The correlation peak is at NT_c=101 chips, as expected.

The sample simulation shown in Figure 6.2 also approximates the ideal cross-correlation performance defined in Section 1 of Chapter 4. The initial results for these single-user C/N values imply that the correlator will perform very well with high reliability for a single transmitted signal in the satellite transponder, as expected.

Next, the results of the multiple access C/I ratios (-20, -22, -24, and -26 dB) are discussed. The results are summarized in Table 6.3.

Received C/N	Detection Rate	Error Rate
-20 dB	87%	13%
-22 dB	61%	39%
-24 dB	33%	67%
-26 dB	18%	82%

Table 6.5. Results of simulation to observe correlation performance for multiple users with an arbitrary data delay. *Detection Rate* is the percentage of correct time delays chosen by the correlator. *Error Rate* is the number of errors divided by the total number of simulations. The simulation parameters were an arbitrary time delay of 80 μs (100 chips), a transmitted m-sequence of length 2046 chips, and an integration time of 2046 chips.

Table 6.3, which shows the required beacon transmit power to achieve the above C/I ratios under different levels of system loading, is shown again for reference as Table 6.6.

		Number of Cellular Users		
		165 users	140 users	83 users
C/I ratios	-20dB	0.25 W	0.25 W	0.1 W
	-22 dB	0.1 W	0.1 W	75 mW
	-24 dB	75 mW	75 mW	50 mW
	-26 dB	50 mW	50 mW	25 mW

Table 6.6. Beacon transmit power levels for simulated C/I ratios at different levels of system loading: maximum capacity (165 users), heavy loading (140 users), and average loading (83 users).

Recall that an incorrect code position is defined as the time delay chosen by the correlator other than the 100 chip time delay. This definition of an error allows the error rate to be defined as the percentage of errors within a set of similar simulations. The results of the simulation at these C/I ratios are unsatisfactory for applications requiring frequent location data information. The detection rate for a C/I ratio of –20 dB may be acceptable for applications only requiring occasional location data information.

For comparison with the single user case shown in Figure 6.1, Figure 6.3 shows a sample output from the correlator for one simulation for a C/I of –26 dB. This C/I ratio corresponds to a 50 mW transmit power with either 165 cellular users or 140 cellular users. (The C/I ratio for a 50 mW transmit power with 140 cellular users is less than 1 dB greater than the C/I ratio for the same transmit power and 165 users.) The results are normalized with respect to the maximum output value.

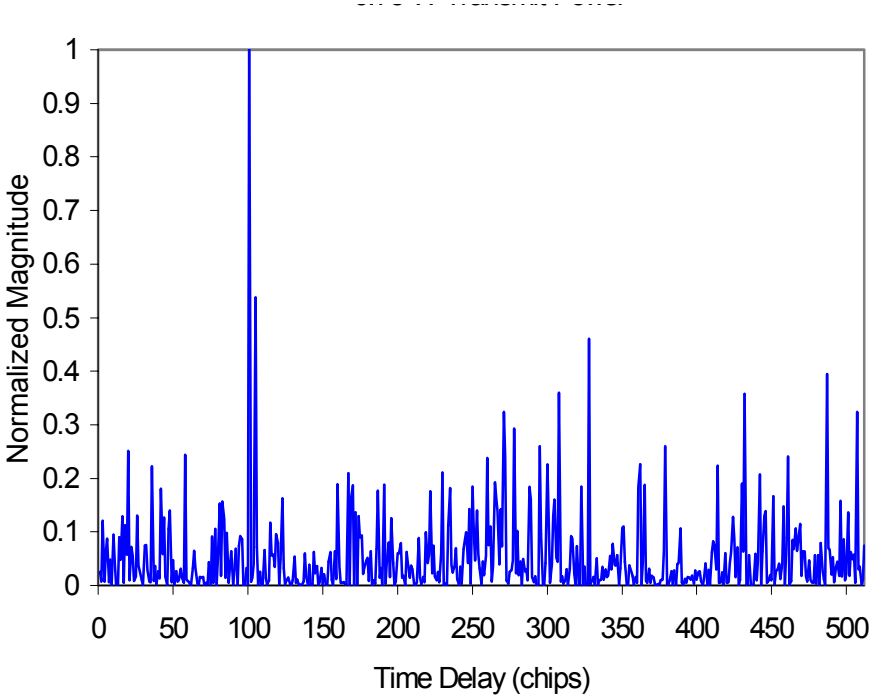

Figure 6.3. Output of correlator for a known code with 100 chip time shift and no Doppler shift. The code length was 2046, the integration time was 512 chips, and the C/I was -26 dB. The user transmit power was 50 mW for 165 simultaneous users in the satellite transponder. The correlation peak is at NT_c=101 chips, as expected.

After observing two separate sets of simulation results, some generalizations can be made about the error rates for the multiple access C/I ratios with the simulation parameters maintained in this group of simulations. The simulation parameters referred to here are the 2046 chip length transmitted m-sequence, the integration time of 2046 chips, some arbitrary time delay, and no Doppler shift.

From the simulation results presented thus far, it can be assumed that (for these simulation parameters) and a C/I of -20 dB, any arbitrary time delay will result in an error rate of approximately 20%. Similar assumptions can be made for the C/I ratios of -22, -24, and –26 dB. These generalizations, including the -20 dB C/I, are summarized in Table 6.7. Refer to Table 6.6 for the beacon transmit power levels and system capacities these results are based on.

Received C/(N+I)	Detection Rate	Error Rate
-20 dB	80%	20%
-22 dB	63%	37%
-24 dB	30%	70%
-26 dB	15%	85%

Table 6.7. Generalized simulation results for tested C/I ratios of correlator performance when the data has an arbitrary time delay. *Detection Rate* is the percentage of correct time delays chosen by the correlator. *Error Rate* is the number of errors divided by the total number of simulations. The simulation parameters were a transmitted m-sequence of length 2046 chips, and an integration time of 2046 chips.

6.2.3 A time delay of 398 chips (0.318 ms)

The last set of simulations performed introduced a 0.318 ms (398 chip) delay to the transmitted m-sequence. The purpose of this group of simulations is to observe the performance of the correlator when an arbitrary time delay is introduced to the transmitted data. The simulation parameters of an m-sequence length of 2046 and an integration time of 2046 chips are maintained. The effects of Doppler shift are not examined in this set of simulations. Rather than comparing the correlator output to a threshold, the maximum output from the correlator was chosen as the correct time alignment.

Only the multiple user ratios (-20, -22, -24, and -26 dB) were examined for this simulation. The results for the worst-case scenario of 165 users in the satellite transponder are presented here. First, a plot of the normalized correlator output (Figure 6.4) from a single multi-user simulation is provided for comparison to the single user results of Figure 6.1. The plot in Figure 6.4 is for a C/I ratio of -24 dB, which corresponds to a 75 mW beacon transmit power with either 165 or 140 cellular users accessing the system at the same time. The C/I ratio for 140 users (heavy loading) is less than 1 dB greater than the C/I ratio for 165 users.

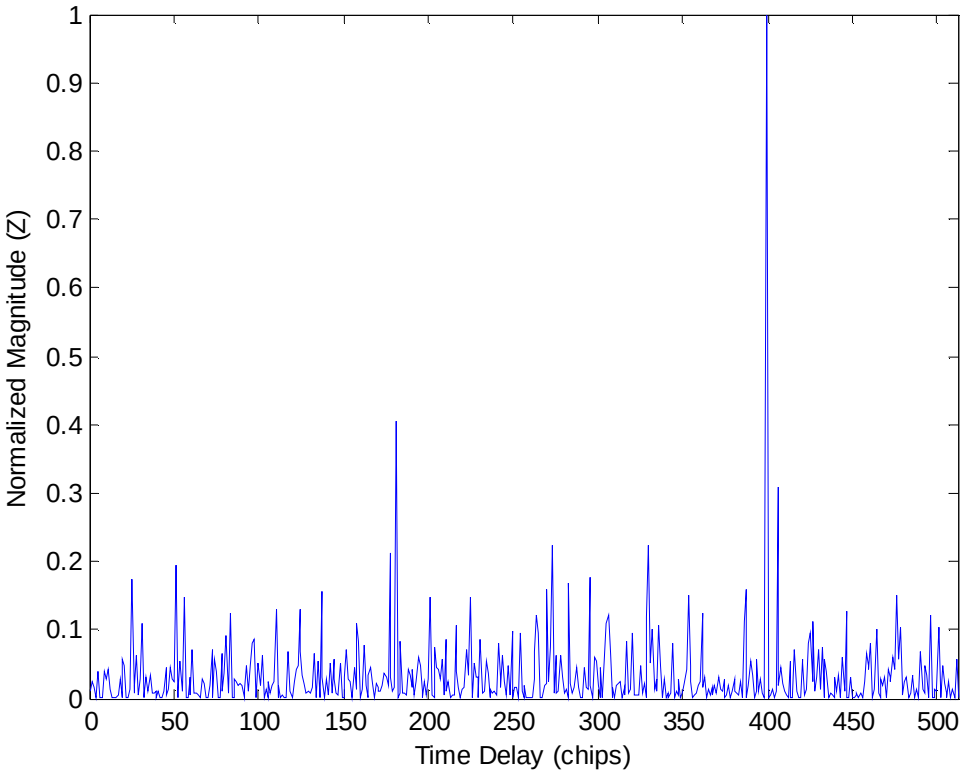

Figure 6.4. Output of correlator for a known code with 398 chip time shift and no Doppler shift. The code length was 2046, the integration time was 512 chips, and the C/I was -24 dB, which corresponds to a transmit power of 75 mW with 165 users in the satellite transponder. The correlation peak is at NT_c=399 chips, as expected.

The primary difference between Figures 6.1 and 6.4 is the level of the correlation noise – the magnitude of the correlations at time delays other than the true time delay. These magnitudes are much larger in Figure 6.4, and correspond to the large interference level relative to the desired transmitted signal. Because the interference component may vary compared to the transmitted signal level, the results in Figure 6.4 are not reliable. The results shown in Figure 6.3 changed with each simulation due to the random nature of the noise.

Table 6.8 summarizes the performance of the correlator for a time delay of 0.318 ms (398 chips) for the C/I ratios of -20, -22, and -24 dB. Since the results were poor for the 100 chip offset at -26 dB, this simulations were not performed for a 398 chip offset. The error rate for a C/I ratio of –26 dB is expected to be the same as the error rate (85%) calculated at other time delays.

Received C/(N+I)	Detection Rate	Error Rate
-20 dB	82%	18 %
-22 dB	61%	39%
-24 dB	33%	67%

Table 6.8. Correlator output statistics for multiple users with an input time delay of 0.318 ms and no Doppler shift. *Detection Rate* is the percentage of correct time delays chosen by the correlator. *Error Rate* is the number of errors divided by the total number of simulations. The simulation parameters were a transmitted m-sequence of length 2046 chips, and an integration time of 2046 chips.

The results summarized in Table 6.8 follow the expected behavior of the correlator described in Table 6.7. As expected, the performance of the correlator decreases as the noise level relative to the transmitted signal increases. As discussed in Chapter 5, performance could be significantly improved by examining all values above a threshold several times. Running the correlator several times at each delay that returns a maximum above the threshold will reduce the noise enough to find the true delay. This stipulation is examined in Section 6.3 by performing a threshold analysis.

6.3 Threshold Analysis

Since the multi-user simulation results for the C/(N+I) ratios of -20, -22, -24, and -26 dB were unsatisfactory for applications requiring frequent location information updates, a threshold analysis was performed to determine if any improvement in performance would result. As discussed in Sections 6.1 and 6.2, the interference power level is much greater than the thermal noise power level and dominates the C/(N+I) ratio. Therefore, the C/(N+I) ratio is referred to as the C/I ratio. The threshold analysis was not performed for the single-user C/N ratios of 0.5, -2.5, -3.7, -5.5, and -8.5 dB.

Several parameters must be defined before the analysis results can be presented. The Probability of Detection (P_D) is defined as the percentage of simulations above a threshold in which the correlator chose the correct time delay. The Probability of False Alarm (P_{FA}) is defined as the percentage of simulations above a threshold in which the correlator did not chose the correct time delay. For readers unfamiliar with threshold analyses, note that the Probability

of False Alarm is not the statistical complement of the Probability of Detection. That is, $P_{FA} \neq 1 - P_D$. The relationship between the Probability of False Alarm and the Probability of Detection is shown in Equation 6.2,

$$P_D = Q_m(\sqrt{2}s, \sqrt{-2\ln(P_{FA})}) \tag{6.2}$$

where Q_m is the Marcum Q-function and is defined in Equation 6.3 as

$$Q_m(a,b) = \int_b^\infty u \exp\left(-\frac{u^2 + a^2}{2}\right) I_o(au)\, du \tag{6.3}$$

and I_o is the zero order Bessel function of the first kind. In Equation 6.2, $s = \sqrt{\frac{PT}{N_o}}$, where *No* is the noise power spectral density, P is the transmitted power, and T is the integration time.

If the output of the correlator for all simulations is not normalized with respect to the maximum output, the range of thresholds required for the analysis will depend on the noise level relative to the transmitted power level. As the relative noise level increases, the threshold range will also increase for data that is not normalized.

Using these definitions, a threshold analysis was performed on the multi-user C/(N+I) ratios. This analysis actually provides more insight into the correlator performance than a threshold analysis on the single-user C/N ratios because very few (if any) errors resulted for these C/N ratios, which was expected. The results of the threshold analysis for the multi-user cases simulated are shown in Figure 6.5.

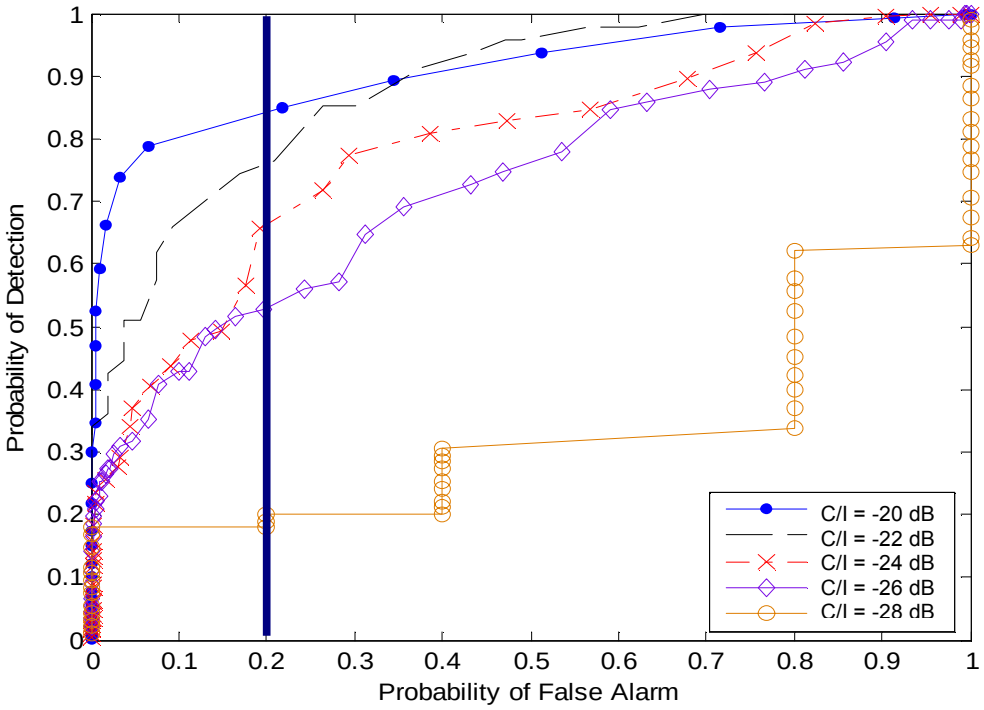

Figure 6.5. Results of Threshold Analysis for multi-user C/I values of -20, -22, -24, -26, and -28 dB. The solid vertical line represents the Probability of False Alarm used in the mean acquisition time analysis below.

The curve for the -28 dB C/I ratio has a stepped nature because there were not enough detections for a good analysis. The results of the –28 dB C/I ratio were not presented in Section 6.2 because the error rate was close to 100%. It is unlikely that the beacon will transmit at power levels below 50 mW, which are required to obtain a –28 dB C/I ratio. The curves in Figure 6.5 approximate the results from theory. The solid vertical line in Figure 6.4 represents the Probability of False Alarm used in the analysis of Mean Acquisition Time.

Mean Acquisition Time is defined as the average time required for the correlator to achieve *lock* on the signal, where lock is defined as the correlator choosing the true signal time delay (and frequency delay). The equation for mean acquisition time is given in Equation 6.4:

$$\bar{T}_{acq} = (C-1)(T_d + P_{fa}T_{fa})\left(\frac{1}{P_d} - \frac{1}{2}\right) + \frac{T_d}{P_d} \qquad 6.4$$

where C is the number of possible time delays (512 chips), T_d is the integration time (2046 chips or 1.64 ms), T_{fa} is the penalty time, and P_{fa} is the probability of false alarm. For this analysis, the probability of false alarm was set at 0.2, and the penalty time was set at $300T_d$, or 0.5 s. The penalty time is defined as the time required for the tracking loop of the correlation circuit to

recognize an incorrect decision and return to the acquisition loop. Using Equation 6.4 and the results from Figure 6.4, the mean acquisition times calculated for the C/I ratios are shown in Table 6.9.

C/I	P_d	T_{acq}
-20 dB	84%	35 s
-22 dB	78%	40.6 s
-24 dB	67%	51.6 s
-26 dB	53%	72 s

Table 6.9. Calculated Mean Acquisition Times for the multi-user C/I ratios, using Equation 6.3. The probability of false alarm was set to 0.2, the penalty time was set at 0.5 s, and the integration time was 1.64 ms. The corresponding probabilities of detection are given.

The beacon transmit power levels required to achieve the C/I ratios of Table 6.9 for different levels of system loading are repeated for reference in Table 6.10. Tables 6.3 and 6.6 contain the same information as Table 6.10.

		Number of Cellular Users		
		165 users	140 users	83 users
C/I ratios	-20dB	0.25 W	0.25 W	0.1 W
	-22 dB	0.1 W	0.1 W	75 mW
	-24 dB	75 mW	75 mW	50 mW
	-26 dB	50 mW	50 mW	25 mW

Table 6.10. Beacon transmit power levels for simulated C/I ratios at different levels of system loading: maximum capacity (165 users), heavy loading (140 users), and average loading (83 users).

Comparing the Probability of Detection values shown in Table 6.9 with the original Detection Rates (shown in Table 6.11) calculated in Section 6.2 shows some improvement for the -20 and -22 dB C/I ratios and significant improvement for the lower C/I ratios. The original Detection Rates from Section 6.2 are shown in Table 6.11 for reference. Table 6.10 gives the beacon transmit power levels required to achieve these C/I ratios under various system loading conditions.

Received C/(N+I)	Detection Rate	Error Rate
-20 dB	80%	20%
-22 dB	63%	37%
-24 dB	30%	70%
-26 dB	15%	85%

Table 6.11. Generalized simulation results for tested C/N ratios of correlator performance when the data has an arbitrary time delay. *Detection Rate* is the percentage of correct time delays chosen by the correlator. *Error Rate* is the number of errors divided by the total number of simulations. The simulation parameters were a transmitted m-sequence of length 2046 chips, and an integration time of 2046 chips. No threshold was used in the decision process.

6.4 Conclusions

The results discussed in this Chapter demonstrate some aspects of the performance of the correlator. From the multiple and single user results presented in this Chapter, the correlator will perform acceptably for a 0.25 W minimum transmit power under worst-case system loading (maximum capacity). If some percentage of error can be tolerated by the application, lower transmit powers can be implemented in the beacon. It can be assumed that the system will not operate under worse-case conditions the majority of the time. If the system is assumed to operate under average load conditions the majority of the time, the minimum required transmit power can be lowered to 0.1 W for acceptable system performance (on average). Some errors or outages may be experienced at a 0.1 W or lower transmit power when the system is operating under maximum capacity loading conditions. Chapter 7 presents the work that remains to be completed in the characterization of this receiver.

Chapter 7

Conclusions

This thesis presented the initial steps in the design of a low power beacon for transmitting location data via the Globalstar Satellite System. The primary goal of this thesis was to determine the minimum beacon transmit power required to achieve a reasonable carrier-to-noise ratio at the receiver (C/N). This minimum transmit power was approximated via a MATLAB simulation. The simulation is only an approximation because of the differences between a Globalstar receiver and the simulated receiver. These differences are discussed in detail in Section 5.2; the key differences resulted from the simplifications made to enable the simulation.

Some of these simplifications were: running the simulator at baseband rather than an IF frequency, not using any forward error correction (FEC) techniques, and neglecting the effect of Doppler shift on the chip rate. Performing the simulations at baseband prevented several aspects of the receiver from being simulated, such as the performance of the matched filter in the correlator (refer to Section 5.2) and the effect of Doppler shift on the carrier frequency. The differences between the Globalstar receiver and the simulated receiver are discussed in more detail in Section 5.2.

The system described in Section 7.1 refers to the transmissions to the Gateway via the satellite within a single satellite footprint (or beam). As discussed in the beginning of Chapter 3, there are 16 beams per satellite in the Globalstar Satellite System. The capacities and corresponding performance results referred to in the discussions below and the discussions of Chapters 5 and 6 refer to a single satellite footprint. The results can be discussed in this manner because the Gateway and the transmitter must lie within the same footprint for a communication link to be established between the two.

7.1 Discussion of Results

The simulation examined two aspects of correlator performance. First the performance of the correlator for a single user was measured; this performance was used to verify the results of the second simulation. The second simulation measured the performance of the correlator for multiple users accessing the satellite transponder at the same time. In both cases, the transmitted signal – or desired transmitted signal in the multi-user case – was shifted in time by an arbitrary time delay. When multiple users are accessing the system at the same time, an interference power level must be added to the thermal noise in the C/N ratio. For the cases considered in the simulations of Section 6.2, the magnitude of the interference is much larger than the magnitude of the thermal noise, and dominates the C/(N+I) ratio. Therefore, the C/(N+I) ratio is referred to as the C/I ratio.

The transmitted signal was an m-sequence of length 2047, and additive white Gaussian noise (AWGN) was added in the channel. The amount of noise added was determined by the C/N ratio at the receiver. The correlator used an integration period of 2047 chips, and the search space was restricted to 512 possible delay positions (in chips). The search strategy was parallel – the maximum output of each correlation was stored, and the position of the largest stored value was selected as the true delay of the transmitted sequence. Three arbitrary time delays were tested in the simulations: 16 μs (20 chips), 80 μs (100 chips), and 0.318 ms (398 chips).

Chapter 3 discusses the Globalstar Satellite System in detail, and Section 3.2.2 presents the Reverse Link budgets for both the uplink (transmissions from the user to the satellite) and the downlink (broadcasts from the satellite to the ground station receiver) for a single user. The differences resulting from multiple users are also discussed.

As discussed above, both single user and multiple user cases were examined in this thesis. For the single user case, the transmit powers tested were 0.75 W and 0.25 W, which correspond to overall C/N ratios of -2.7dB and –8.5 dB. For the multiple user case, C/I ratios examined were -20 dB, -22 dB, -24 dB, and -26 dB for different levels of system loading. Three levels of system loading were considered: maximum capacity (165 cellular users), heavy loading

(140 cellular users), and average loading (83 cellular users). Different beacon transmit power levels were required under the various system loads to achieve these C/I ratios. Section 7.1.1 discusses these values. These C/I ratios were used in the receiver simulation because they dominate the C/(N+I) ratio, as discussed in Chapter 3.2.2.

Performance of the correlator was quantified by the calculated detection rate. The detection rate for these simulations is defined as the number of simulations in which the correlator chose the correct time delay divided by the total number of simulations. The error rate is the complement of the detection rate. Both rates were determined from within a set of simulations with the same C/N or C/I ratio *and* time delay. The correlator did not perform well at the multiple access C/I ratios less than –22 dB. As expected, the single user simulations resulted in excellent correlator performance.

In Section 6.3, a threshold analysis is presented for the multi-user C/I ratios (-20, -22, -24, -26, and -28 dB). The threshold analysis adapts the original decision methodology by comparing the output of the correlator at each time delay to a threshold. The value (or values) that exceeds the threshold is chosen as the true time delay. The threshold is varied over the range of correlator outputs in order to plot the Probability of False Alarm vs. Probability of Detection Curve in Figure 6.4. This curve is significant because it shows that for very low C/I ratios (below –24 dB), significant performance improvement can be obtained by selecting the proper threshold.

7.1.1 Comparison of Results

The results of the simulations in Chapter 6 showed that for a given C/N ratio, the likelihood of the receiver determining the correct code delay converged to a percentage. This likelihood was determined by calculating the percentage of simulations that resulted in the correct code delay for each set of test parameters. Table 7.1 summarizes the beacon transmit powers that correspond to the C/I ratios for different system loading conditions, and Table 7.2 summarizes the C/I ratios and the corresponding percentage of simulations that returned the correct code delay.

		Number of Cellular Users		
		165 users	140 users	83 users
C/I ratios	-20dB	0.25 W	0.25 W	0.1 W
	-22 dB	0.1 W	0.1 W	75 mW
	-24 dB	75 mW	75 mW	50 mW
	-26 dB	50 mW	50 mW	25 mW

Table 7.1. Beacon transmit power levels for simulated C/I ratios at different levels of system loading: maximum capacity (165 users), heavy loading (140 users), and average loading (83 users).

Received C/I	Detection Rate	Error Rate
-20 dB	80%	20%
-22 dB	63%	37%
-24 dB	30%	70%
-26 dB	15%	85%
-28 dB	5%	95%

Table 7.2. Correlator detection statistics for multiple users for a transmitted m-sequence of length 2047 chips and various C/N ratios. The correlator used an integration time of 2047 chips and examined 512 delay positions (in chips) during each correlation. *Detection Rate* is the number of correct code positions divided by the total number of simulations. *Error Rate* is the number of errors divided by the total number of simulations.

The results from the threshold analysis show that significant performance improvement can be obtained for very low C/N ratios (below –24 dB). These results are summarized in Table 7.3. Table 7.1 provides the corresponding beacon transmit power levels.

C/N	P_d	T_{acq}
-20 dB	84%	35 s
-22 dB	78%	40.6 s
-24 dB	67%	51.6 s
-26 dB	53%	72 s
-28 dB	20%	234 s

Table 7.3. Threshold analysis results for a transmitted m-sequence of length 2047chips and various C/N ratios. The correlator used an integration time of 2047 chips and examined 512 delay positions (in chips) during each correlation. *Detection Rate* is the number of correct code positions divided by the total number of simulations. *Detection Rate* is the number of correct code positions divided by the total number of simulations. *Error Rate* is the number of errors divided by the total number of simulations.

7.1.2 Application of Results

The single user case analyzed in Section 6.1 presents an ideal scenario for system operation. This scenario is not likely to occur, but provides insight into the operation of the system. The three cases analyzed for multiple user loading show average, above-average, and worst-case system performance. The maximum capacity of a single satellite footprint is 165

users. This thesis assumed a heavy load of 85% capacity (140 users) and an average load of 50% capacity (83 users). The number of users accessing the satellite may be much lower than 83 users at night (or after normal business hours) or when the satellite is being under-utilized.

The multiple user access results presented in Section 7.1 show that a minimum transmit power of 0.25 W is required to achieve satisfactory system performance under maximum system capacity conditions (165 users). For system conditions at 50% capacity (83 users), a minimum transmit power of 0.1 W is required to achieve satisfactory performance. For applications requiring only occasional location information updates, lower power levels may provide acceptable system performance.

As discussed in Section 6.3, system performance could be improved by changing the search strategy in the correlator. A parallel search could still be used, but a threshold should be implemented. Examining each correlation that exceeds the threshold – rather than simply choosing the maximum value resulting from all correlations – would improve detection performance.

7.2 Future Work

More work needs to be done in order to determine the parameters required for optimum system performance. First, the simulation should be converted to run at an IF frequency so the effects of the Doppler shift on the carrier frequency and the code clock rate can be observed and quantified. A matched filter bank [42] needs to be implemented after the correlator to complete the design of the receiver as shown in Section 1 of Chapter 5. An FFT can be used to implement the matched filter bank in MATLAB. A Rake receiver should also be implemented to improve correlator performance. Rake receiver operation is discussed in Section 4.2.1, and the interested reader should refer to [5, 20, 35] for more information.

Once Doppler shift is simulated, non-coherent integration should be implemented in the correlator; coherent integration is currently implemented in the correlator. In coherent

integration, one integral is performed over the entire integration period. In non-coherent integration, several shorter integrations are summed to integrate the entire data stream. Non-coherent integration could improve performance when the signal frequency offset is larger than the reciprocal of the integration time – that is, when $\Delta f \geq \frac{1}{NT_c}$. Non-coherent and coherent integration is discussed in more detail in Section 5.3.

After these simulations are complete, coding should be added to the transmitted data signal. The Globalstar system utilizes Convolutional encoding, which should be simulated first. Turbo coding should also be simulated to determine if any additional gain can be obtained. A demodulator will also need to be implemented in the simulation to recover the data and determine the bit error rates for uncoded versus coded data streams. The bit error rate is the number of bit errors relative to the bit energy to noise ratio and is a primary measure of the performance of a communication system.

Finally, the reduction of the search space needs to be examined. This work does not examine the optimum search space, but this parameter needs to be examined closely. Chapter 5 discusses the reduction of the search space; one method of reduction is discussed in [54]. Properly minimizing the search space would significantly reduce the acquisition time of the correlator by removing improbable time and frequency combinations, thereby reducing the number of possible false detections.

Bibliography

1. Aston, P.S. *Satellite telephony for field and mobile applications*. in *2000 IEEE Aerospace Conference Proceedings. Big Sky, MT*. 2000.
2. Axonn LLC. *AXTracker*. 2005 [cited 2005 September 22]; Available from: http://www.axonn.com.
3. Bacon, P. *Introduction to Globalstar satellite communication system*. in *IEE Colloquium on Communication Opportunities Offered by Advanced Satellite Systems* 1998. London, UK: IEE.
4. Berrou, C., A. Glavieux, and P. Thitimasjshima. *Near Shannon Limit Error-Correcting Coding and Decoding: Turbo-Codes*. in *Proceedings of the IEEE International Conference on Communications*. 1993. Geneva, Switzerland: IEEE.
5. Bottomley, G.E., T. Ottosson, and Y.E. Wang, *A Generalized RAKE Receiver for Interference Suppression.* IEEE Journal on Selected Areas in Communications, 2000. **18**(8): p. 1536-1545.
6. Buehrer, Michael R. *Class Lecture.* ECE 5660: Spread Spectrum Communications. Virginia Tech, Spring 2006.
7 Capuzzello, A., et al. *The integration of Globalstar satellite system with the GSM terrestrial network*. in *Proceedings of Fourth European Conference on Satellite Communications*. 1997. Rome, Italy.
8. Chang, D.D. and O.L. de Weck, *Basic capacity calculation methods and benchmarking for MF-TDMA and MF-CDMA communication satellites.* International Journal of Satellite Communications and Networking, 2005. **23**: p. 153-171.
9. Crowe, K., *A Comparative Analysis of the Iridium and Globalstar Satellite Transmission Paths*. 1999, Air Force Institute of Technology, Wright-Patterson AFB. p. 220.
10. De Gaudenzi, R., F. Giannetti, and M. Luise, *Advances in Satellite CDMA Transmission for Mobile and Personal Communications.* Proceedings of the IEEE, 1996. **84**(1): p. 18-39.
11. Dietrich, F.J., *The Globalstar Cellular Satellite System.* IEEE Transactions on Antennas and Propagation, 1998. **46**(6): p. 935-942.
12. Dietrich, F.J. *The Globalstar satellite cellular communication system: design and status*. in *Proceedings of UCSD WC '98 1st Annual UCSD Conference on Wireless Communications. San Diego, CA*. 1998.
13. Dixon, R.C., *Spread Spectrum Systems with Commercial Applications*. Third Edition ed. 1994, New York: John Wiley & Sons, Inc.

14. Europa Technologies Ltd. *GSM Coverage Map.* 2005 [cited September 17 2005]; Available from: http://www.coveragemaps.com/press/EuropaPress_GSM_EuropeanMap2006A.htm

15. Evans, J., *Satellite Systems for Personal Communications*, in *IEEE Antennas and Propagation Magazine*. 1997. p. 7-20.

16. Fossa, C., *A Performance Analysis of the IRIDIUM Low Earth Orbit Satellite System*. 1998, Air Force Institute of Technology, Wright-Patterson AFB. p. 113.

17. Fossa, C.E., et al. *Overview of the IRIDIUM low earth orbit (LEO) satellite system*. in *Proceedings of the 1998 IEEE National Aerospace and Electronics Conference, NAECON*. 1998: IEEE.

18. Frieden, R. *Assessing the scope of global personal communication services*. in *Proceedings of 16th Annual Pacific Telecommunications Conference. Honolulu, HI*. 1994.

19. Glisic, S.G., R.L. Pickholtz, and W. Wu, *Issues in CDMA Applications for Mobile LEO Satellite Communications.* IEEE, 1996.

20. Glisic, S.G., et al., *Design Study for a CDMA-Based LEO Satellite Network: Downlink System Level Parameters.* IEEE Journal on Selected Areas in Communications, 1996. **14**(9): p. 1796-1808.

21. Globalstar. *Simplex Transmitter Unit*. 2005 [cited 2005 September 22]; Available from: http://www.globalstar.com.

22. Glover, I.A. and P.M. Grant, *Digital Communications*. 1998: Prentice Hall.

23. Golovanevsky, L., et al. *Globalstar link verification*. in *IEEE Wireless Communications and Networking Conference*. 1999. New Orleans, LA.

24. Guichon, T. *G-SENS STx INTEGRATION MANUAL*. Rev 8. AeroAstro Inc. August 15, 2003

25. Harada, H. and R. Prasad, *Simulation and Software Radio for Mobile Communications*. 2002, Boston, MA: Artech House.

26. Hendrickson, R. *Globalstar for military applications*. in *Proceedings of IEEE Military Communications Conference (MILCOM'00)*. 2000. Los Angeles, CA: IEEE.

27. Hirshfield, E., *The Globalstar System: Breakthroughs in Efficiency in Microwave and Signal Processing Technologies.* Space Communications, 1996. **14**(2): p. 69-82.

28. Hollis, R. *Mobile satellite services*. in *Proceedings of 17th Annual Pacific Telecommunication Conference (Convergence: Closing the Gap). Honolulu, HI*. 1995.

29. Huber, J.F., *Satellite mobile communication: Satellite mobile networks with global radio coverage promise to be the market of the future.* Telcom Report (English Edition), 1994. **17**(6): p. 8-11.

30. Ibnkahla, M., ed. *Signal Processing for Mobile Communications Handbook*. 2005, CRC Press: Boca Raton.

31. Inmarsat. *Maritime Coverage Map*. 2005 [cited 2005 September 22]; Available from: http://support.inmarsat.com/coverage/maritime_coverage_map.aspx.

32. Jaynes, T. *Development of an Aeronautical Inmarsat D+ Terminal*. in *Proceedings of SPIE*. 2000: IEEE.

33. Kakavas, I., *The Applications in Military Communications of Low and Medium Earth Orbit Commercial Satellite Systems*. 1997, Naval Postgraduate School: Monterey, CA. p. 144.

34. Lian, K.J., *Adaptive Antenna Arrays for Satellite Personal Communication Systems*. 1997, Virginia Polytechnic Institute and State University: Blacksburg, VA. p. 115.

35. Liu, H. and K. Li, *A Decorrelating RAKE Receiver for CDMA Communications Over Frequency-Selective Fading Channels.* IEEE Transactions on Communications, 1999. **47**(7): p. 1036-1045.

36. Maine, K., Devieux, C., Swan, P. *Overview of IRIDIUM Satellite Network.* in *Proceedings of the 1995 Wescon Conference.* 1995. San Francisco, CA: IEEE.

37. Mazzella, M., et al. *Multiple access techniques and spectrum utilisation of the GLOBALSTAR mobile satellite system*. in *Fourth IEE Conference on Telecommunications*. 1993. Manchester, UK: IEE.

38. McNeff, J.G., *The Global Positioning System.* IEEE Transactions on Microwave Theory and Techniques, 2002. **50**(3): p. 645-652.

39. Meenan, C., R. Tafazolli, and B. Evans. *Intelligent paging schemes for non-GEO satellite personal communication networks*. in *1997 IEEE 47th Vehicular Technology Conference. Technology in Motion. Phoenix, AZ.* 1997.

40. Monte, P. and S. Carter. *The Globalstar Air Interface: Modulation and Access*. in *Proceedings of 15th AIAA International Communication Satellite Systems Conference*. 1994. San Diego, CA: IEEE.

41. NAL Research Corp. *Iridium Satellite Modem, Model A3LA-DGS.* 2005 [cited 2005 August 30]; Available from: http://www.nalresearch.com.

42. Persson, B., D.E. Dodds, and R.J. Bolton. *A segmented matched filter for CDMA code synchronization in systems with Doppler frequency offset*. 2001.

43. Pickholtz, R.L., D.L. Schilling, and L.B. Milstein, *Theory of Spread-Spectrum Communications - A Tutorial.* IEEE Transactions on Communications, 1982. **COM-30**(5): p. 855-884.

44. Porcino, D. *Location of Third Generation Mobile Devices: A Comparison between Terrestrial and Satellite Positioning Systems*. in *IEEE Vehicular Technology Conference*. 2001. Rhodes, Greece: IEEE.

45. Pratt, T., C. Bostian, and J. Allnutt, *Satellite Communications*. Second ed. 2003, Hoboken, NJ: John Wiley & Sons. 536.

46. Schiff, L. *Signal Design and System Operation of Globalstar versus IS-95 CDMA - simularities and differences*. in *Proceedings of ICUPC '97*. 1997. San Diego, CA: IEEE.

47. Schiff, L. *System operation for IS-95 terrestrial vs. Globalstar-similarities and differences*. in *Proceedings of ICUPC 97 - 6th International Conference on Universal Personal Communications. San Diego, CA*. 1997.

48. Skywave Mobile Communications. *DMR-200 D*. 2005 [cited 2005 August 30]; Available from: http://www.skywavemobile.com.

49. Sprint Nextel. *Sprint PCS International Roaming*. 2005 [cited 2005 September 14]; Available from: http://www1.sprintpcs.com/explore/coverage/internationalroaming/Search.jsp.

50. Stenger, D.K., *Survivability analysis of the iridium low earth orbit satellite network*. 1996, Air Force Institue of Technology, Wright-Patterson AFB. p. 77.

51. Stone, C., *Integration of Commercial Mobile Satellite Services into Naval Communications*. 1997, Naval Postgraduate School: Monterey, CA. p. 167 p.

52. Trimble. *Trimtrac*. 2005 [cited 2005 September 22]; Available from: http://www.trimtrac.com.

53. Tronche, C. *Satellite system for multimedia and mobile telecommunications*. in *28th European Microwave Conference Proceedings. Amsterdam, Netherlands. 6-8 Oct. 1998.* 1998.

54. Vardoulias, G., *Receiver synchronisation techniques for CDMA mobile radio communications based on the use of a priori information*. 2000, University of Edinburgh: Edinburgh. p. 180.

55. Wang, C., D. Sklar, and D. Johnson. *Forward Error-Correction Coding*. Crosslink 2002 [cited 2006 February 18]; Available from: http://www.aero.org/publications/crosslink/winter2002/04.html.

56. Ween, A., et al. *GSM signalling for prioritised military LEOs communications*. in *MILCOM 97 MILCOM 97 Proceedings. Monterey, CA*. 1997.

57. Wells, P. *Military use of global mobile personal communications systems*. in *IEE Colloquium on Military Satellite Communications. London, UK. IEE. 6 June 2000.* 2000.

58. Wiedeman, R.A. *The role of GLOBALSTAR, a satellite-based personal communications system, in the wireless revolution*. in *Proceedings of 15th Pacific Telecommunications Conference (PTC '93). Honolulu, HI*. 1993.

59. Wiedeman, R.A. and A.J. Viterbi. *The Globalstar mobile satellite system for worldwide personal communications*. in *Proceedings of 3rd International Mobile Satellite Conference. Pasadena, CA*. 1993.

60. Yoder, T.L., *The use of Iridium, a commercial telecommunications satellite system, in wartime*. 1996, U.S. Army Command and General Staff College: Fort Leavenworth, Kan. p. 98.